Diffraction from polycrystalline materials

Paolo Scardi

Department of Materials Engineering and Industrial Technologies
University of Trento

Paolo.Scardi@unitn.it

CONTENTS

PART I

- From single-crystal to powder diffraction
- Intensity scattered from a powder sample

PART II

- Features and aberrations of the powder geometry
- Structure factor and intensity calculations

Diffraction and Reciprocal lattice

A vector drawn from the origin of the reciprocal lattice to the point (*hkl*), where *h*, *k*, *l* are the Miller indices (integer numbers) is given by:

$$\underline{d}^*_{hkl} = h\underline{a}^* + k\underline{b}^* + l\underline{c}^*$$

where $\underline{a}^*$, $\underline{b}^*$, $\underline{c}^*$ are the reciprocal space vectors

The vector modulus is the inverse of the interplanar distance for the planes with indices (*hkl*):

$$d^*_{hkl} = \left|\underline{d}^*_{hkl}\right| = \frac{1}{d_{hkl}}$$

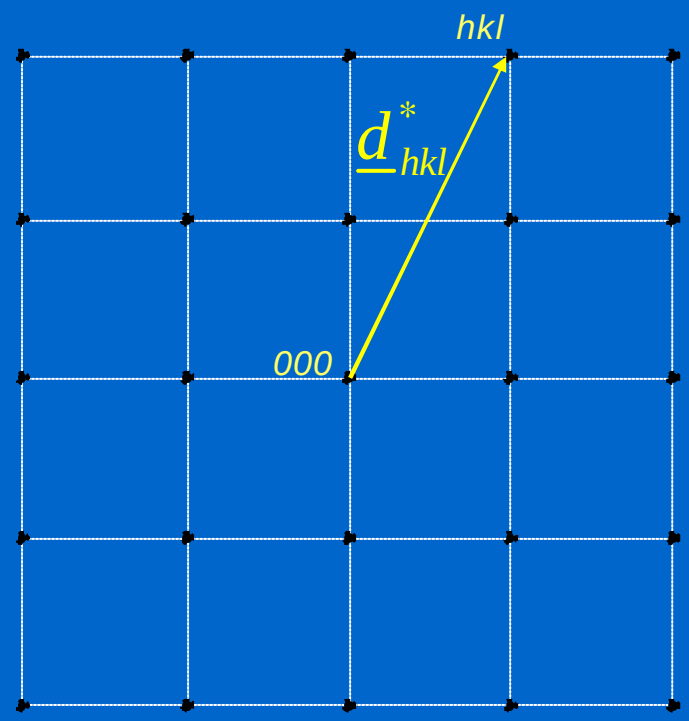

Diffraction and Reciprocal lattice

Versors $\underline{s}_0$ and $\underline{s}$ identify, respectively the incident and scattered beam

$$\left|\frac{\underline{s}-\underline{s}_0}{l}\right| = \frac{2\sin q}{l} = \frac{1}{d} = d^*$$

$$d^*_{hkl} = \left|\underline{d}^*_{hkl}\right| = \frac{1}{d_{hkl}}$$

$\underline{d}^*$ = *scattering vector*

The Bragg law in reciprocal lattice is

$$\frac{\underline{s}-\underline{s}_0}{l} = \underline{d}^*_{hkl}$$

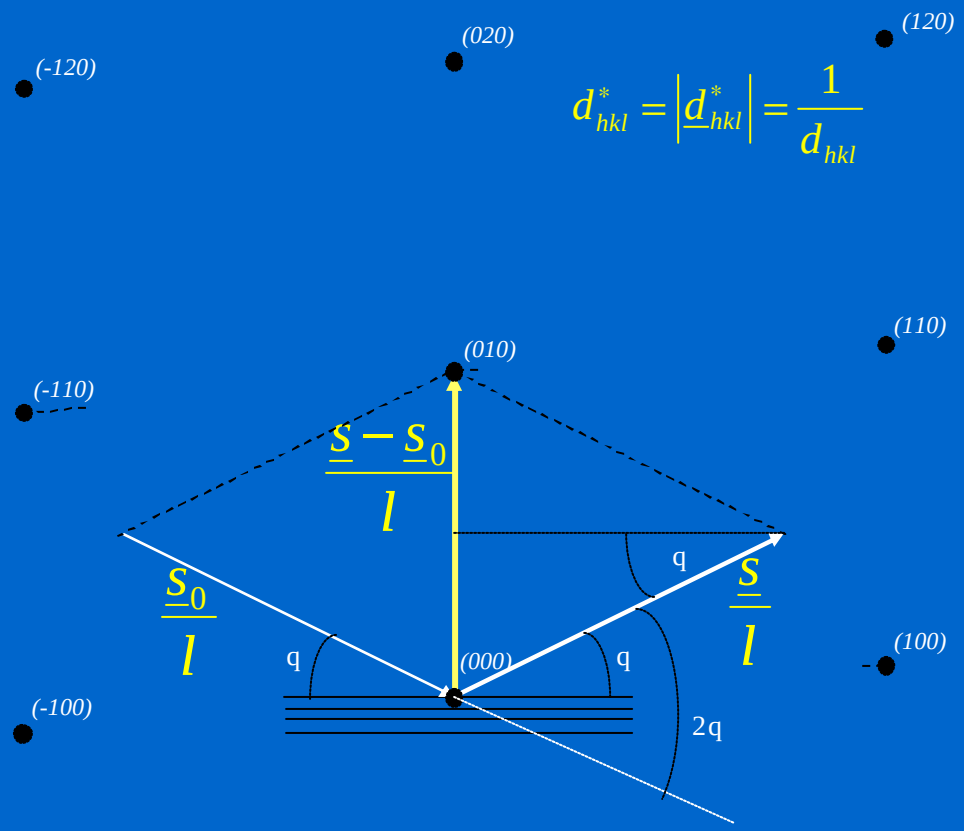

DIFFRACTION AND RECIPROCAL SPACE

For a ***perfect (infinite) crystal***

The ***reciprocal lattice*** is made of (infinitely small) points representing sets of planes of Miller indices *hkl*

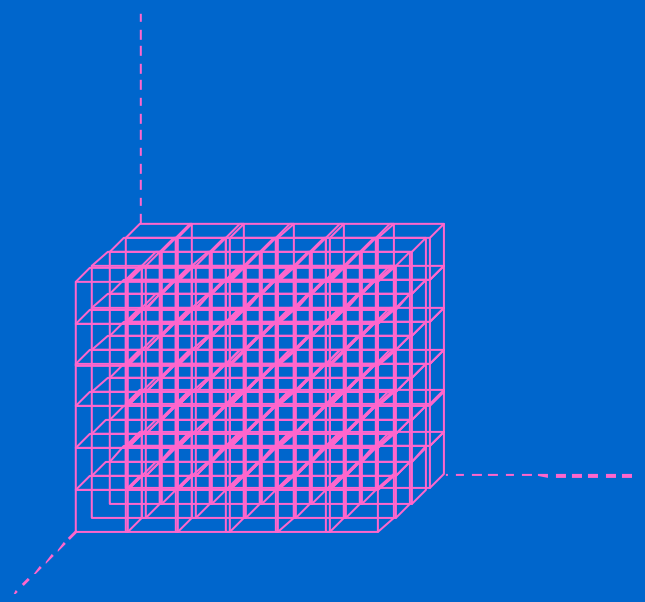

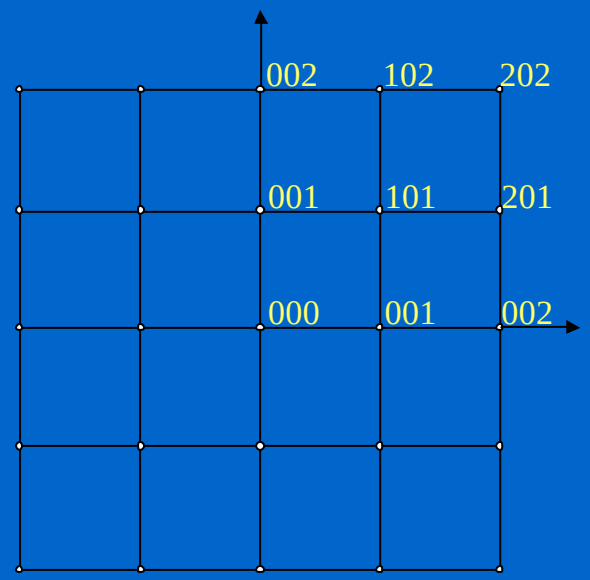

DIFFRACTION AND RECIPROCAL SPACE

For a ***perfect (infinite) crystal*** the **peak width** is determined by the instrumental resolution only:

$$|\underline{s}-\underline{s}_0| = \frac{2\sin q}{l} = \frac{1}{d_{hkl}} = d^*_{hkl}$$

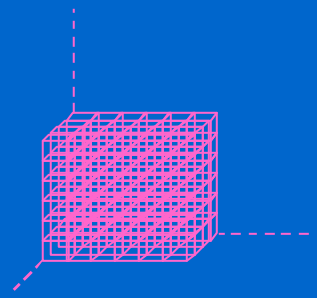

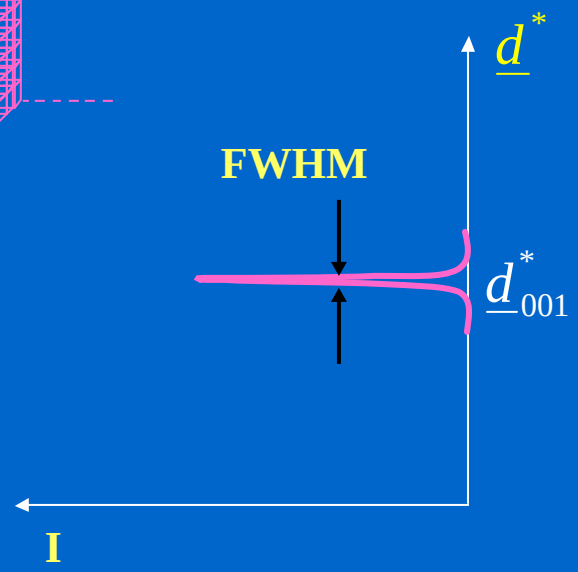

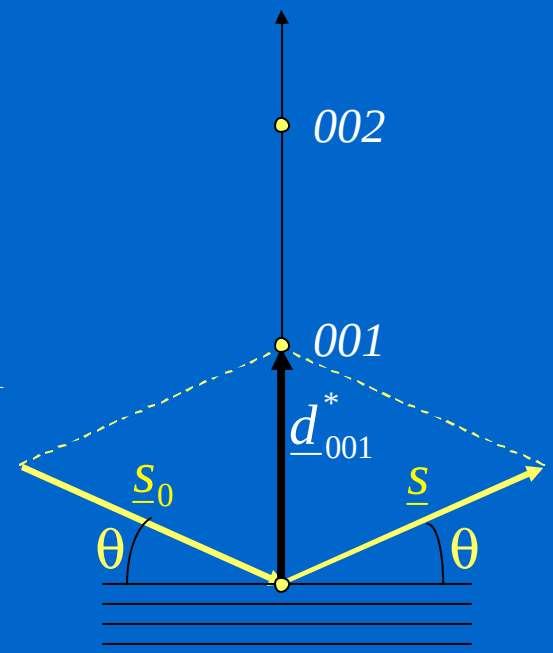

DIFFRACTION AND RECIPROCAL SPACE

For a ***finite crystal (L<1mm)***

Reciprocal lattice points have finite extension. The shape is related to the crystal shape .

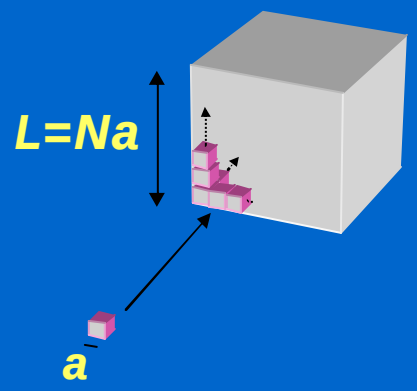

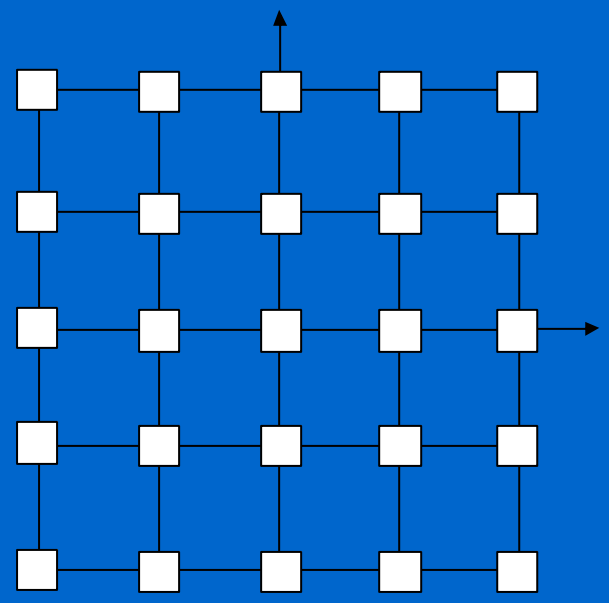

DIFFRACTION AND RECIPROCAL SPACE

Integral breadth: $b\left(d^*\right) = \dfrac{Peak\ Area}{Peak\ Maximum} = \dfrac{1}{L}$ *(Scherrer formula)*

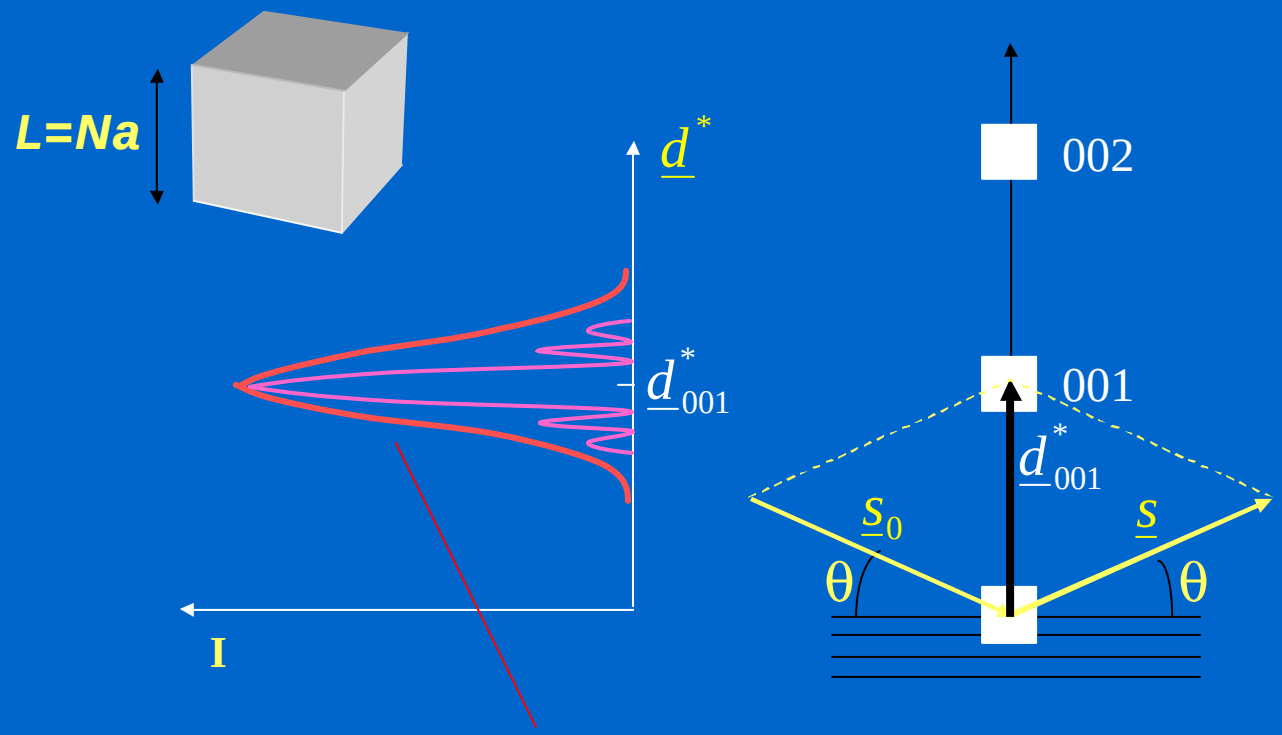

Effect of instrument, domains with different shape/size

RECIPROCAL LATTICE: DIFFRACTION CONDITIONS

For a given wavelength, the Bragg law sets a limit to the interplanar distances for which diffraction is observed:

$$\sin q = l/2d \leq 1$$

$$d^* \leq \frac{2}{l}$$

All points representing planes that can diffract are inside a sphere of finite radius, ***2/l***
(limiting sphere)

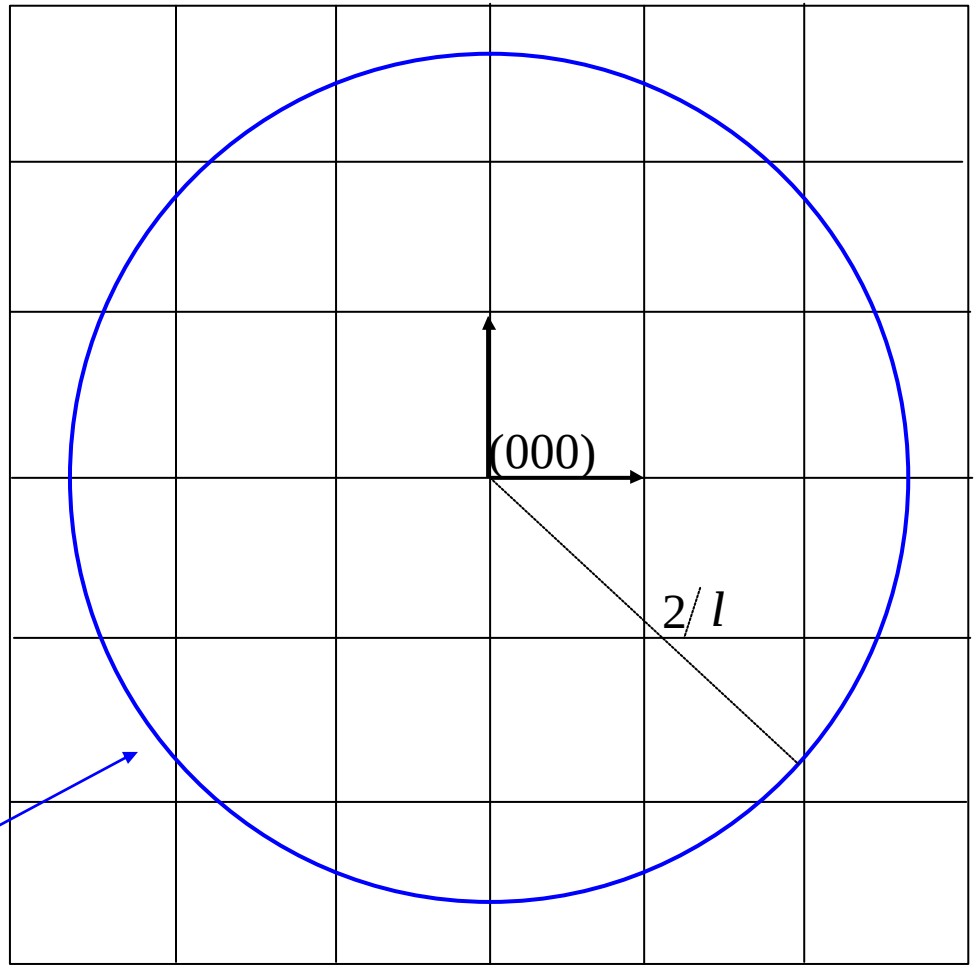

RECIPROCAL LATTICE: DIFFRACTION CONDITIONS

Diffraction conditions occur when the tip of the scattering vector ***d**** falls on a point of the reciprocal space.

The condition is fulfilled by all points on the ***Ewald sphere***, a sphere of radius 1/λ, tangent to the origin and to the 2/λ sphere.

In a powder diffraction measurement, the Ewald sphere can be thought as *rotating* inside the 2/λ sphere.

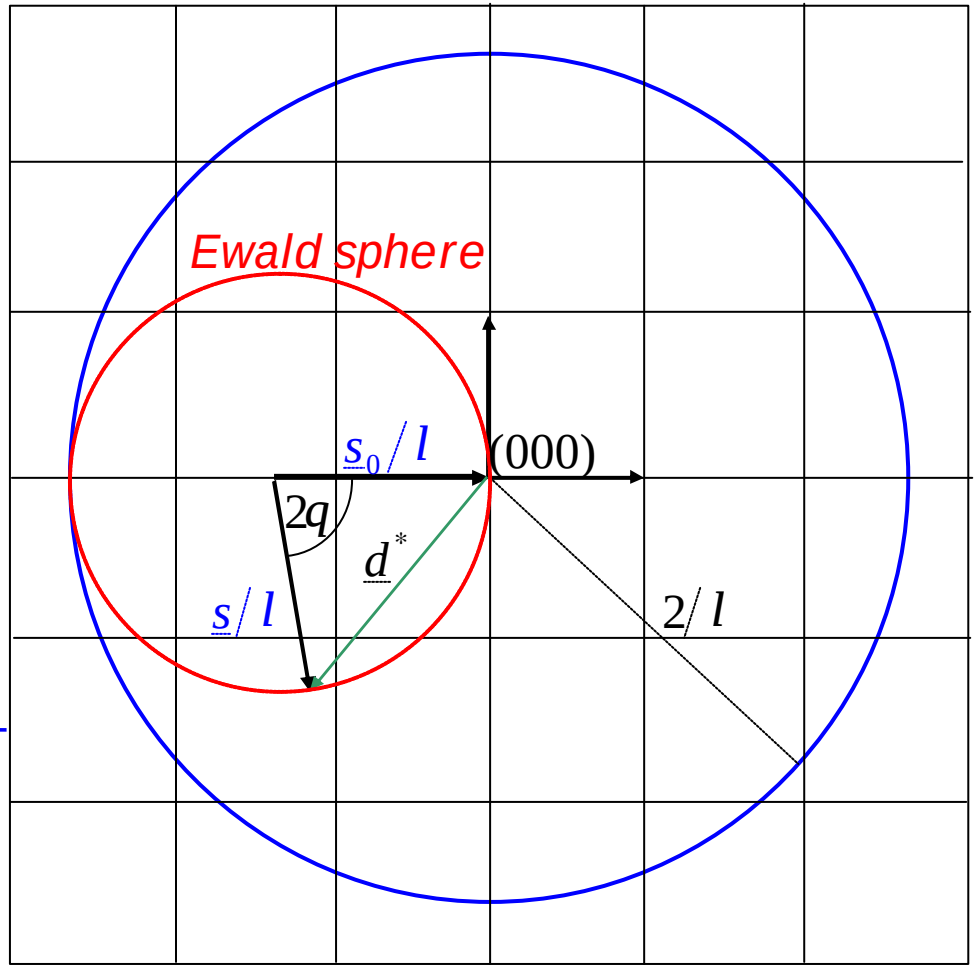

RECIPROCAL LATTICE: DIFFRACTION CONDITIONS

As a consequence, the tip of the scattering vector 'sweeps' the surface of a ***sphere of radius d****

During a powder diffraction measurement, the sphere of radius ***d**** swells (for increasing 2θ) and sweeps the reciprocal space within the limits:

$$0 \le d^* \le \frac{2}{l}$$

$$(0 \le 2q \le 180°)$$

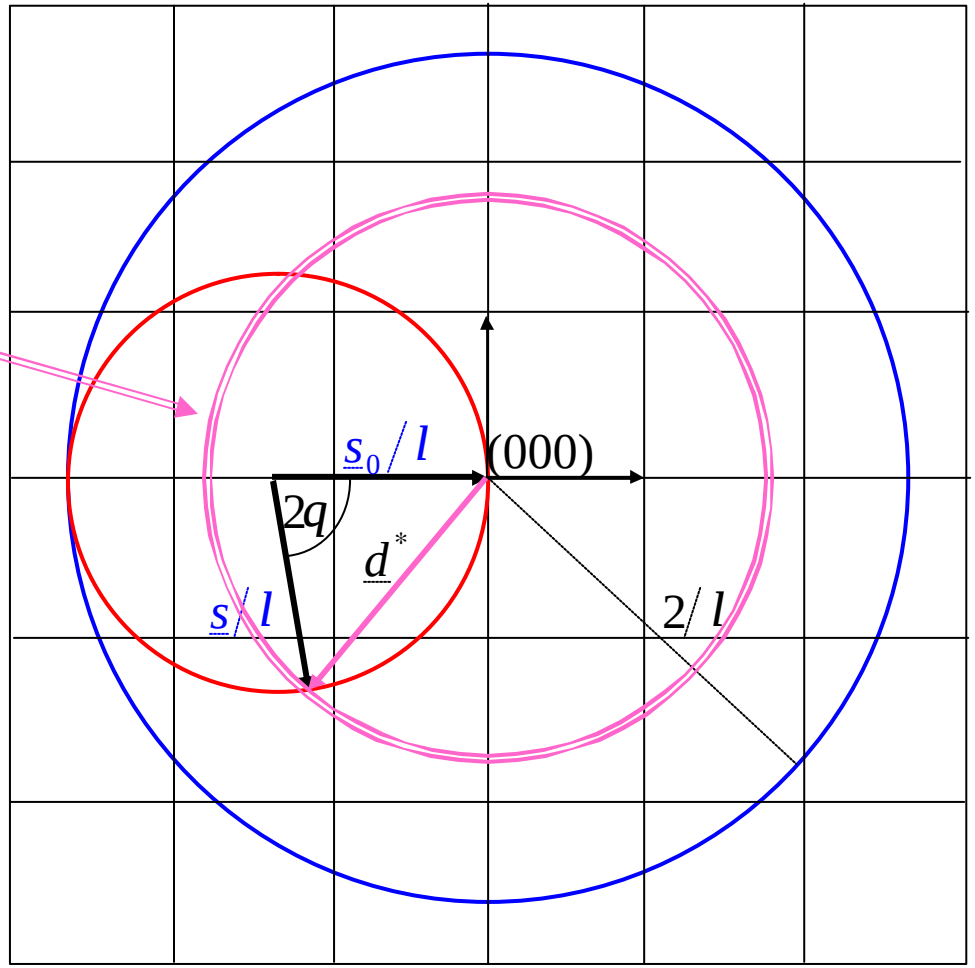

RECIPROCAL LATTICE: POWDER DIFFRACTION

Diffraction takes places whenever the scattering vector crosses a reciprocal space point (*hkl*):

$$\frac{\underline{s}-\underline{s}_0}{l}=\underline{d}^*_{hkl}$$

In a powder diffraction measurement, the sphere of radius ***d**** progressively 'swells' (increasing 2θ) and sweeps the reciprocal space within the limiting sphere:

All reciprocal space points on the PD sphere are in diffraction condition (→ multiplicity).

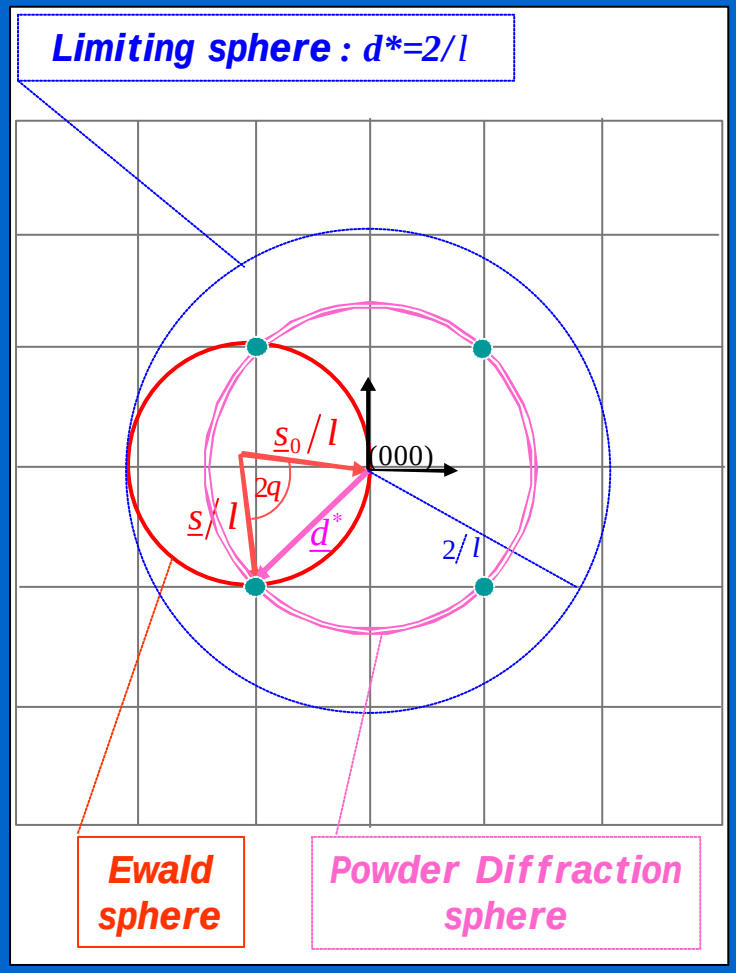

RECIPROCAL LATTICE: MULTIPLICITY

In a powder (polycrystalline material) measurement, several points can be in diffraction condition ***simultaneously***, i.e., for the same 2θ.

This property is expressed by the concept of ***multeplicity*** of a diffraction peak, i.e., the number of equivalent planes.

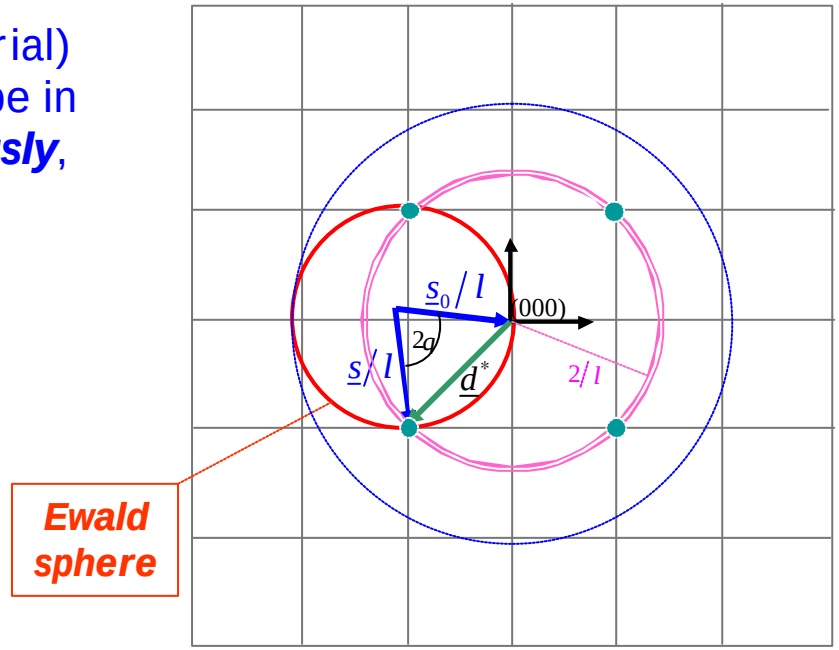

In cubic structures:

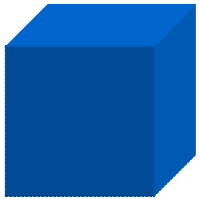

Miller indices	*hkl*	*hhk*	*0kl*	*0kk*	*hhh*	*00l*
Multeplicity	48	24	24	12	8	6

CONTENTS

PART I

- From single-crystal to powder diffraction
- Intensity scattered from a powder sample

PART II

- Features and aberrations of the powder geometry
- Structure factor and intensity calculations

The concept of 'Powder'

An ideal powder is a polycrystalline sample (a true powder or a bulk specimen) such that for every possible orientation a sufficiently high number of grains (→ ***grain statistics***) has atomic planes in Bragg condition (***random orientation***).

If preferred orientations (***texture***) are present, suitable models are necessary to account for the 'non-ideal' conditions.

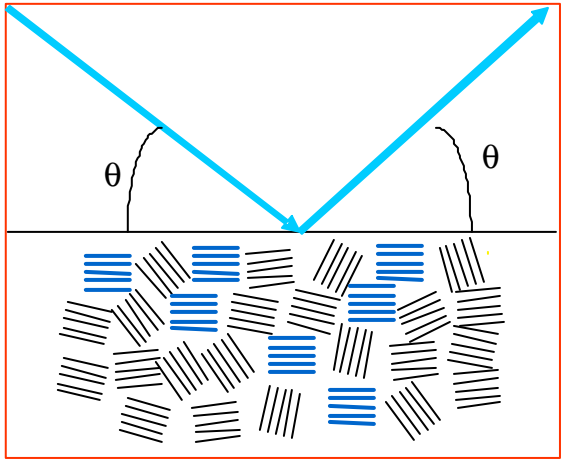

Random orientation

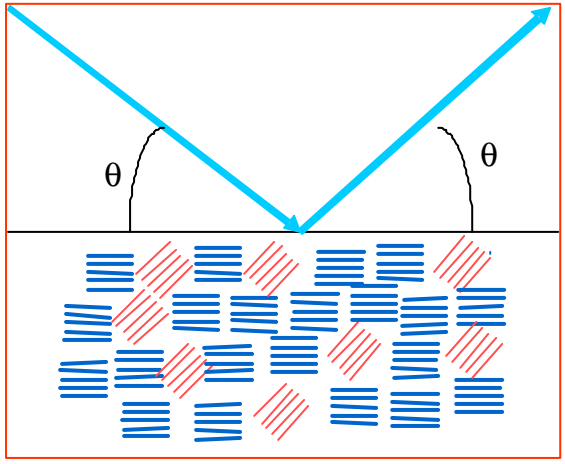

Preferred orientation

Integrated intensity

Intrinsic features of the sample, instrument and measurement geometry cause a dispersion of the scattered intensity across a finite angular range (***a peak***). The range (width) changes with $2q$.

The diffracted signal is better represented by the area of the diffraction peak (***integrated intensity)*** than by maximum intensity.

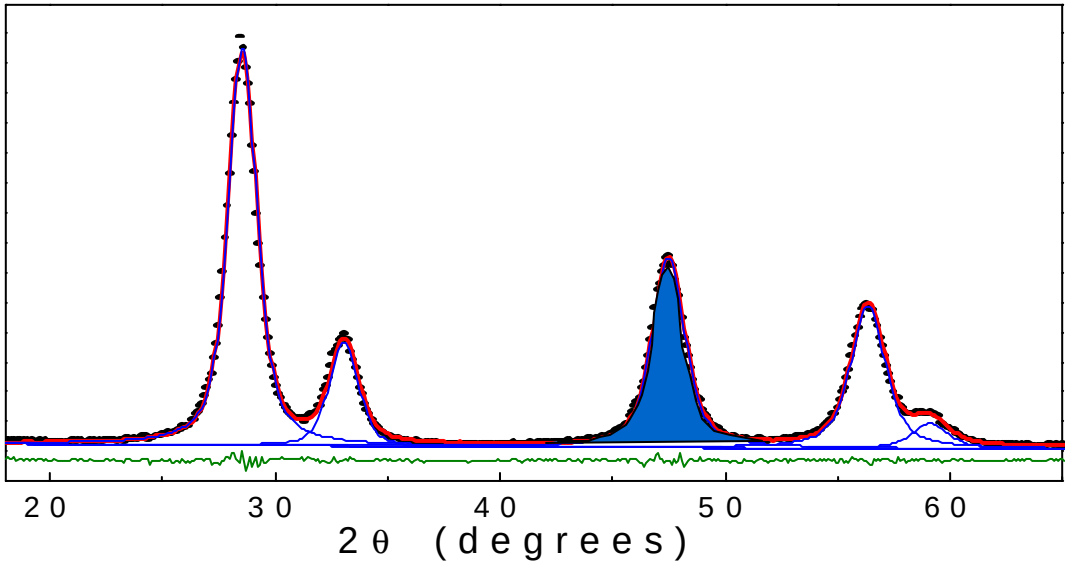

INTEGRATED INTENSITY

The ***integrated intensity*** of a powder diffraction peak is given by:

$$I(2q) = k'|F_T|^2 \, p \left(\frac{1+\cos^2(2q)}{\sin(q)\sin(2q)} \right)$$

Structure factor

Molteplicity

Lorentz-Polarization factor

INTEGRATED INTENSITY

A diffraction measurement basically consists in a cross section through one or more reciprocal space (RS) points.

The measured intensity depends on:

a) The way RS points are crossed;

b) The sampling in RS (considering measurements are in $2q$ space);

c) The fraction of diffracted signal collected by the detector.

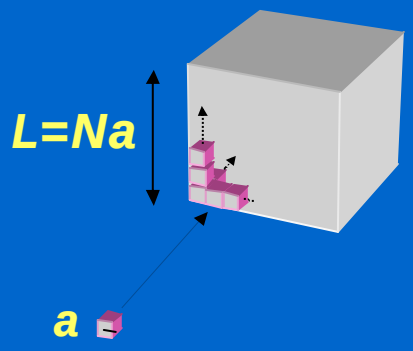

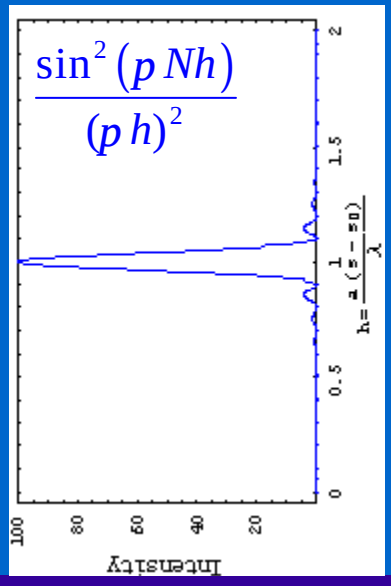

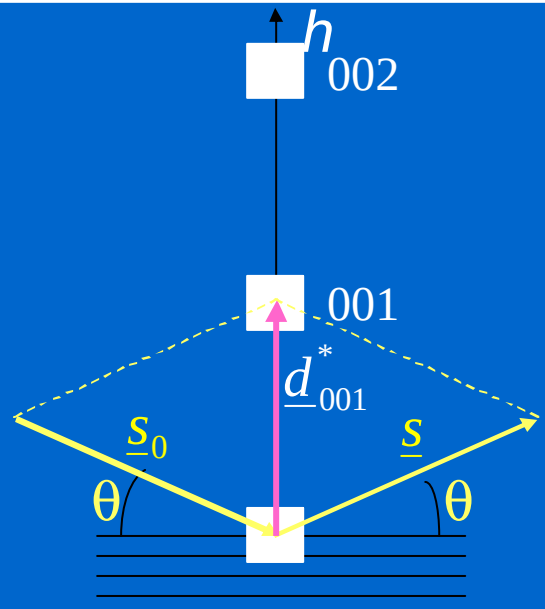

THE LORENTZ FACTOR

Points a), b), c) give the so-called *Lorentz factor*, which depends on the diffraction geometry. As for the way an *hkl* point in RS is "***crossed***" during a measurement, the effect is:

$$\propto 1/\sin(2q)$$

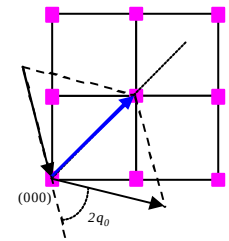

The fraction of crystalline domains whose planes are in diffraction condition changes with the *2q* angle. This fraction is proportional to the ratio between a stripe of width *rDq* and the total surface of the sphere.

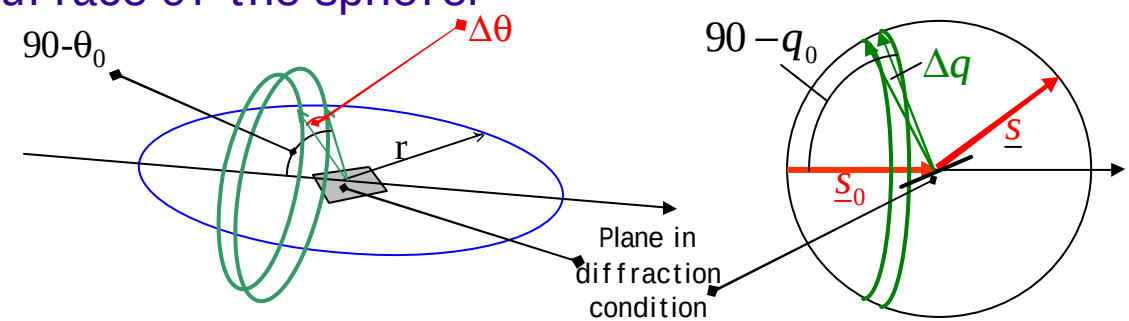

This feature gives a term $\propto \cos(q)$

THE LORENTZ FACTOR

Finally, as shown in the figure below, during a traditional powder diffraction measurement, the X-ray detector spans just a portion (h) of the base circle of the diffraction cone.

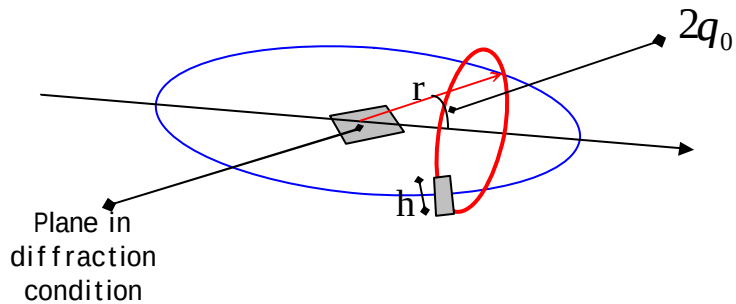

This gives a further trigonometric term, proportional to the integrated intensity: $\propto 1/\sin(2q)$

THE LORENTZ FACTOR

Putting together the trigonometric terms described so far, we obtain the ***Lorentz Factor*** for the powder geometry:

$$LF = \frac{1}{\sin 2q} \cdot \cos q \cdot \frac{1}{\sin 2q} = \frac{\cos q}{\sin^2 2q}$$

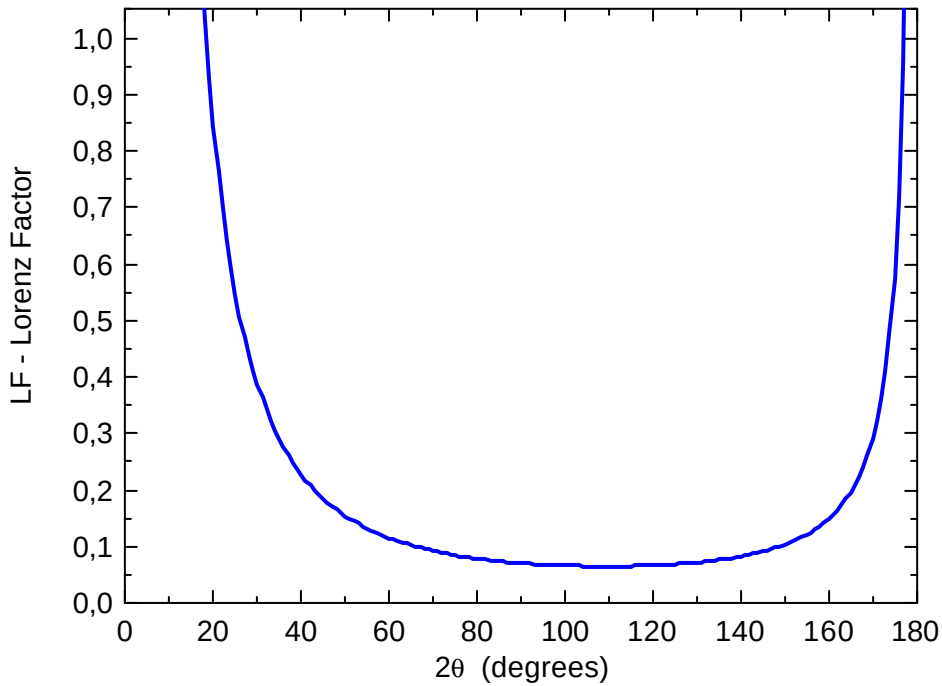

POLARIZATION FACTOR

An additional trigonometric term is in the ***Polarization Factor*** :

$$PF = \left[1 + \cos^2(2q)\right] / 2$$

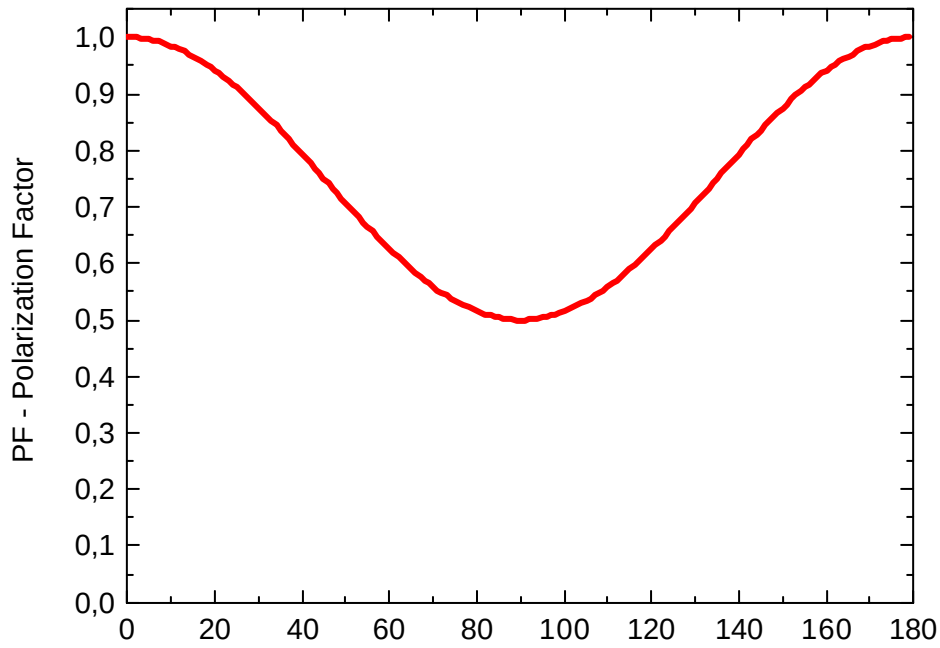

THE LORENTZ-POLARIZATION FACTOR

The Lorentz and Polarization factors can be combined in a single trigonometric term: the ***Lorentz-Polarization*** factor:

$$LF = \frac{\cos q}{\sin^2 2q} \qquad PF = \left[1+\cos^2(2q)\right]/2 \quad \Longrightarrow \quad \boxed{LP = \frac{1+\cos^2(2q)}{\sin(q)\sin(2q)}}$$

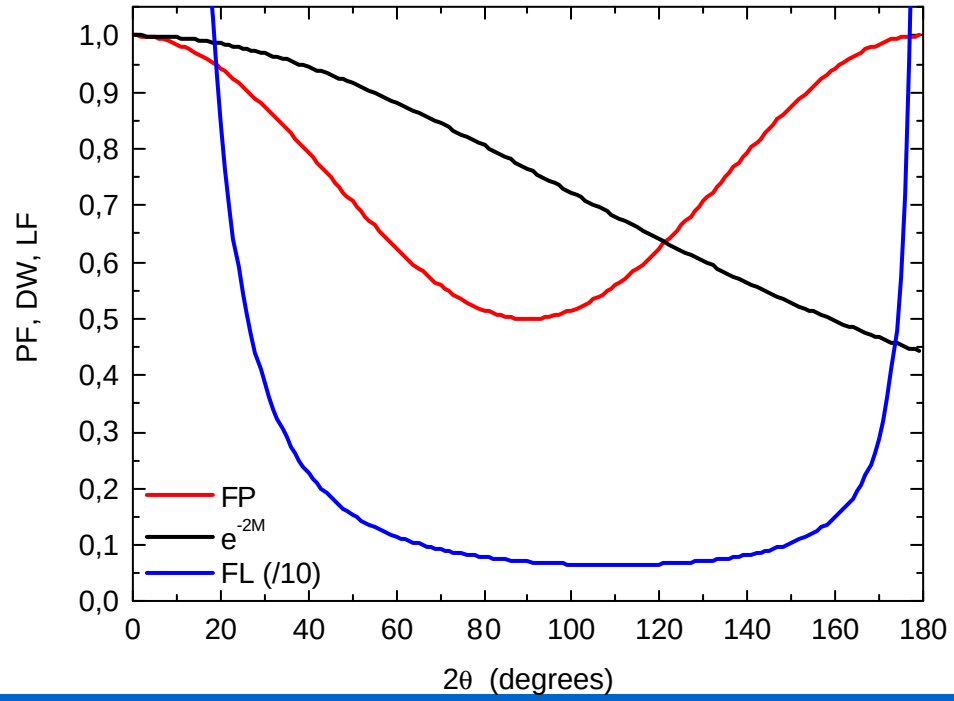

ABSORPTION

One of the main advantages of the traditional powder diffraction geometry (Bragg-Brentano) is that it does not require q-dependent correction terms for the absorption of the X-rays.

Consider a beam with cross section $\boldsymbol{A_0}$ and intensity $\boldsymbol{I_0}$ impinging with an angle q_1. A small volume ***dV***, with thickness ***dx*** and surface $A_0/\sin(q_1)$ diffracts at the angle q_2.

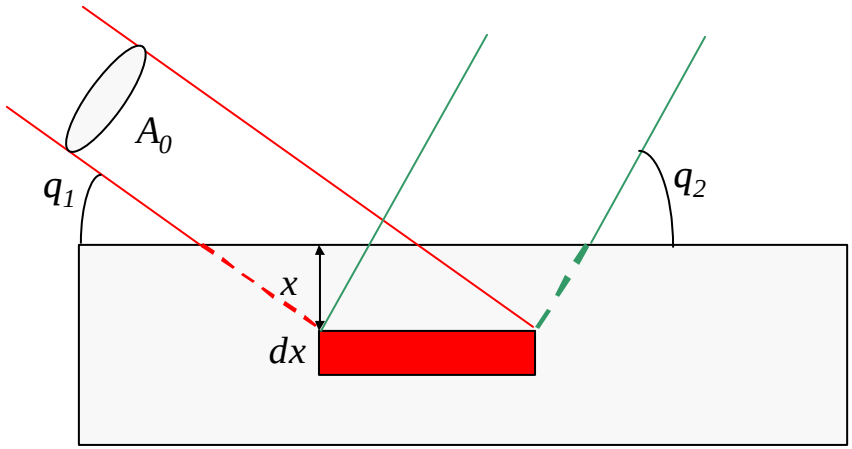

$$dI = I_0 e^{-mx(1/\sin q_1 + 1/\sin q_2)} dV = \frac{I_0 A_0}{\sin q_1} e^{-mx(1/\sin q_1 + 1/\sin q_2)} dx$$

ABSORPTION

$$dI = I_0 e^{-mx(1/\sin q_1 + 1/\sin q_2)} dV = \frac{I_0 A_0}{\sin q_1} e^{-mx(1/\sin q_1 + 1/\sin q_2)} dx$$

In the traditional powder geometry: $q_1 = q_2 = q$

By integrating on the sample thickness: $I = \frac{I_0 A_0}{\sin q} \int_0^\infty e^{-2mx/\sin q} dx = \frac{I_0 A_0}{2m}$

Indipendent of q

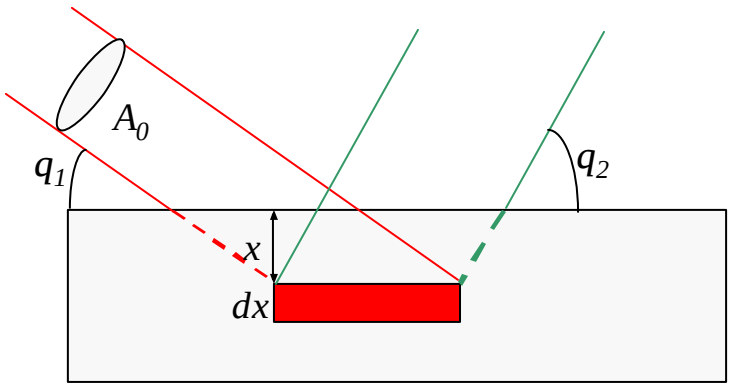

INTEGRATED INTENSITY

If terms for absorption (m), cell volume (v_a), goniometer radius (r) and wavelenght (l) are written explicitly, $k' = k\, l^3 / m r v_a^2$

$$I(2q) = k \frac{l^3}{m r v_a^2} |F_T|^2 \, p \left(\frac{1+\cos^2(2q)}{\sin(q)\sin(2q)} \right)$$

Structure factor

Molteplicity

Lorentz-Polarization factor

INTEGRATED INTENSITY

If the secondary circle of a crystal monochromator (analyzer) is present at q_m, the polarization factor must be written as:

$$I(2q) = k' \frac{|F_T|^2 \, l^3 p}{m r v_a^2} \left(\frac{1+\cos^2(2q_m)\cos^2(2q)}{\sin(q)\sin(2q)} \right)$$

Structure factor

Absorption

Molteplicity

Lorentz-Polarization factor

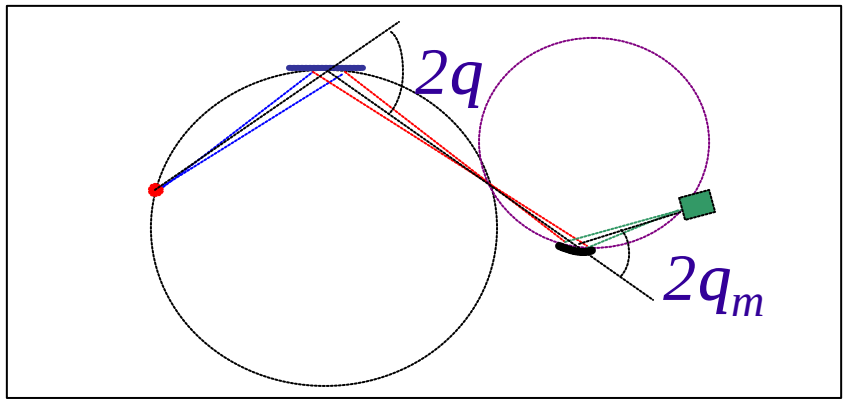

CONTENTS

PART I

- From single-crystal to powder diffraction
- Intensity scattered from a powder sample

PART II

- Features and aberrations of the powder geometry
- Structure factor and intensity calculations

BRAGG-BRENTANO GEOMETRY

H.P. Klug & L.E. Alexander, *X-ray Diffraction procedures*, Wiley, New York, 1974

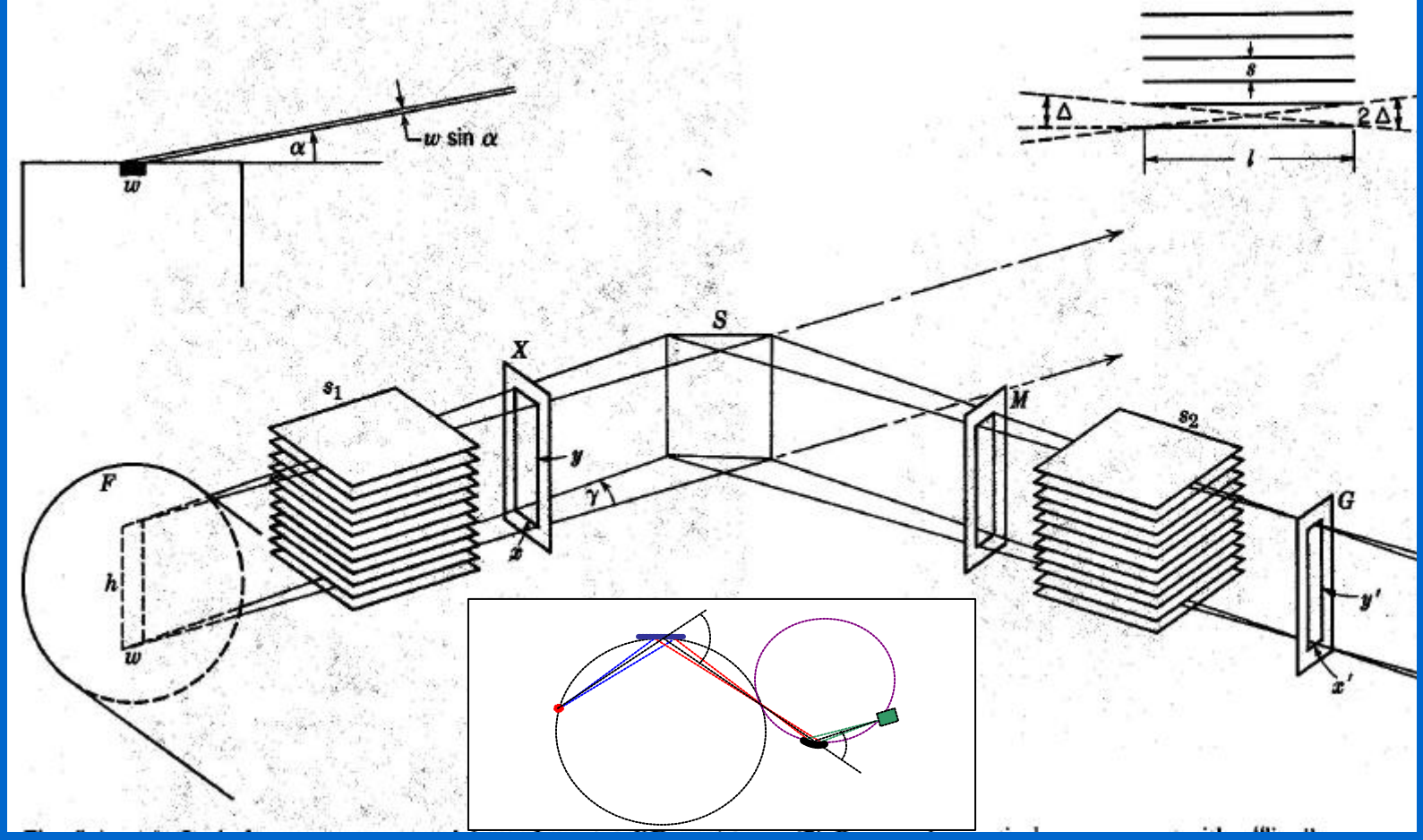

DIFFRACTION PROFILE IN THE POWDER GEOMETRY

The instrumental profile results from a ***convolution*** of several effects:

$$g = g_I \otimes g_{II} \otimes g_{III} \otimes g_{IV} \otimes ....$$

The main contributions are those due to:

- Emission profile
- Flat sample
- Axial Divergence
- Sample transparency
- Receiving slit

.....

DIFFRACTION PROFILE IN THE POWDER GEOMETRY

H.P. Klug & L.E. Alexander, *X-ray Diffraction procedures*, Wiley, New York, 1974

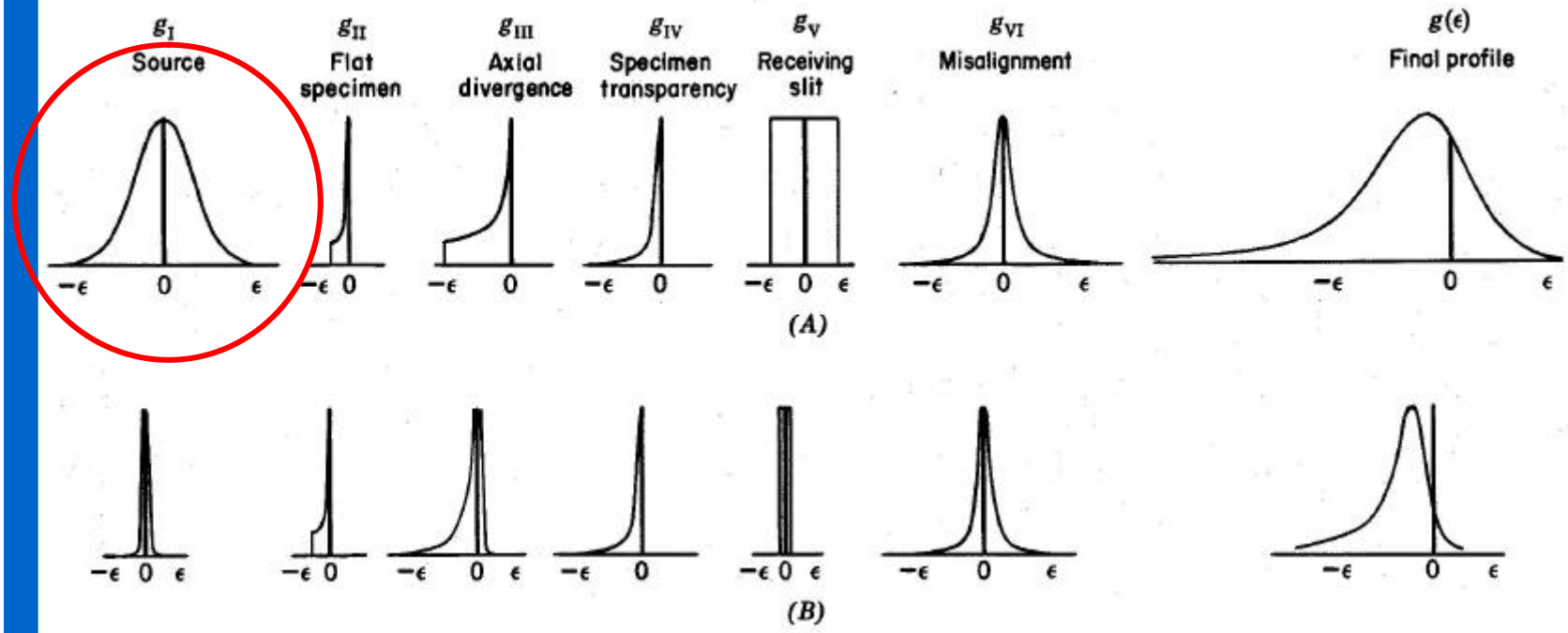

$$g = g_I \otimes g_{II} \otimes g_{III} \otimes g_{IV} \otimes ....$$

EMISSION PROFILE

Emission profile: the Ka_1/Ka_2 doublet:

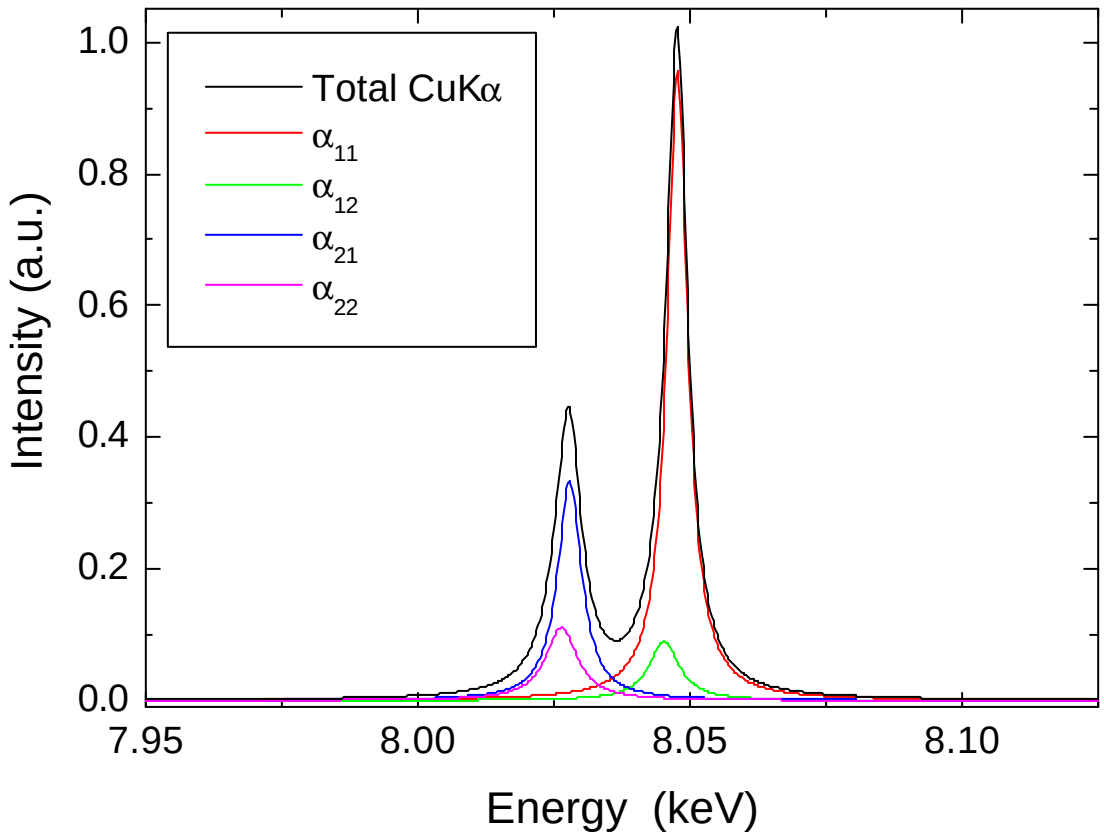

Cu Ka emission profile as modelled by four Lorentzians

EMISSION PROFILE

Line width (G), asymmetry (k) and emission energy (E) for the Kα components of Cu, Cr, Fe, Co. Note that two average Kα components are most frequently used instead of the four in the previous figure

	$K\alpha_1$			$K\alpha_2$		
	E (keV)	Γ (eV)	κ	E (keV)	Γ (eV)	κ
Cu	8.048	2.56	1.12	8.028	4.05	1.10
Cr	5.415	2.16	1.38	5.406	2.75	1.18
Fe	6.404	2.35	1.43	6.391	2.84	1.25
Co	6.930	2.87	1.32	6.915	3.59	1.25

EMISSION PROFILE

Cu Kα emission spectrum with two components (a). FWHM of the emission spectrum ($K\alpha_1$ component) as a function of the diffraction angle, 2θ) (b).

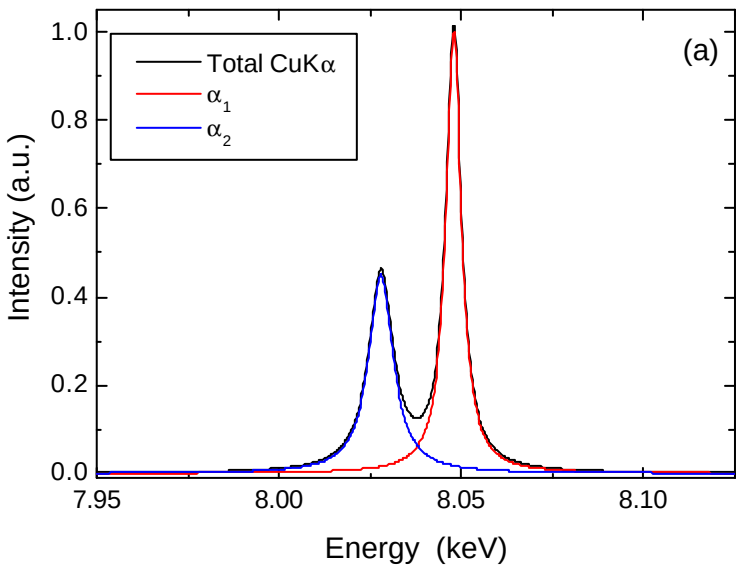

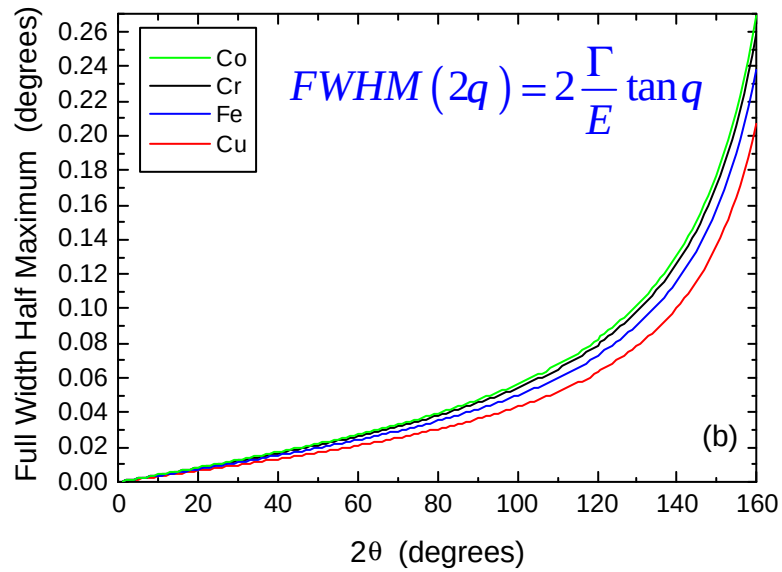

$$l = \frac{c}{n} = \frac{ch}{E} = \frac{12398}{E} \qquad \left|\frac{dl}{l}\right| = \left|\frac{dE}{E}\right| = \frac{2d\cos q \cdot dq}{2d\sin q} = \frac{d(2q)}{2\tan q} \qquad \Rightarrow \quad d(2q) = 2\left|\frac{dE}{E}\right|\tan q$$

INTEGRAL BREADTH

In addition to peak position, maximum and integrated intensity, a useful quantity is the ***integral breadth*** (b), defined as the ratio between peak area and maximum intensity.

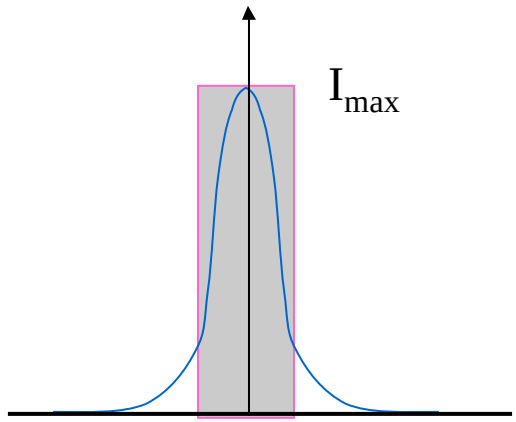

Relation between integral breadth in reciprocal space and $2q$ space

$$b\left(2q\right) = b\left(d^{*}\right) \cdot \frac{l}{\cos q}$$

ANALYTICAL PROFILE FITTING

Nowadays, the most popular data processing programs make use of ***analytical profile fitting***. The basic algorithm (even though not the only one, probably not always the best) adopts a non-linear least squares (NLLS) minimization engine.

The quantity to minimize is:

$$S_y^2 = \sum w_i^2 \left[y_{i,o} - y_{i,c} \right]^2$$

where $y_{i,o}$ and $y_{i,c}$ are respectively the observed and calcualted intensities, whereas the weight is $w_i = 1/\sqrt{y_{i,o}}$.

Calculated (model) intensities, $y_{i,c}$, are typically described by bell-shaped analytical curves, like:

Gaussian, Lorentzian, pseudo-Voigt, Voigt or Person VII functions.

ANALYTICAL PROFILE FITTING

Analitycal profile functions commonly used in peak profile fitting:

$$x = 2q - 2q_0 \; or \; d^* - d^*_{hkl}$$

$$G(x, b_G) = I_o \cdot \exp\left(-\frac{p\,x^2}{b_G^2}\right) \qquad C(x, b_C) = \frac{I_o}{1 + \frac{p^2 x^2}{b_C^2}}$$

$$pV(x) = I_o\left[(1-h)\cdot G(x, b_G) + h \cdot C(x, b_C)\right] =$$

$$= I_o\left[(1-h)\cdot \exp\left(-\frac{p\,x^2}{b_G^2}\right) + h \cdot \frac{1}{1 + \frac{p^2 x^2}{b_C^2}}\right]$$

ANALYTICAL PROFILE FITTING

Useful properties of the ***pV*** function are, e.g., that the IB is simply given by:

$$b_{pV} = (1-h)\, b_G + h b_C$$

if G and C components of the pV have the same width (HWHM). It is also possible to use 'Split ***pV***', with right (R) and left (L) HWHMs:

$$pV(x) = I_o \cdot \left[(1-h) \cdot \exp\left(-\ln(2) \frac{x^2}{w_{L,R}^2} \right) + h \cdot \frac{1}{1 + \frac{x^2}{w_{L,R}^2}} \right]$$

ANALYTICAL PROFILE FITTING

Fit quality is typically expressed by suitable statistical quality indices:

$$S_y^2 = \sum_i w_i^2 \left[y_{i,o} - y_{i,c} \right]^2$$

$$R_{wp} = \left\{ S_y^2 \Big/ \sum_i w_i^2 y_{i,o}^2 \right\}^{1/2}$$

$$R_{\exp} = \left[(N - P) \Big/ \sum_i w_i y_{i,o}^2 \right]^{1/2}$$

$$GoF = R_{wp} / R_{\exp}$$

where ***N*** is the number of data points, ***P*** is the number of fit parameters.

ANALYTICAL PROFILE FITTING

H.P. Klug & L.E. Alexander, *X-ray Diffraction procedures*, Wiley, New York, 1974

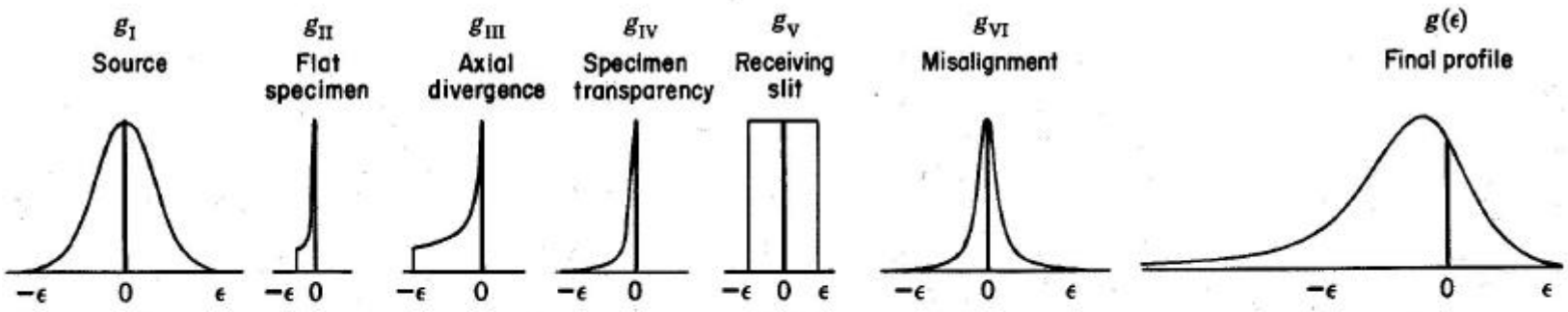

$$g = g_I \otimes g_{II} \otimes g_{III} \otimes g_{IV} \otimes ....$$

The observed profile (*h*) is a convolution of the ***instrumental profle*** (*g*) with the ***'true' diffraction profile*** due to microstructure and lattice defects of the studied sample (*f*)

$$h(h) = f(h-e) \otimes g(e)$$

f profile → small crystalline domain size, dislocations, faulting, etc.

ANALYTICAL PROFILE FITTING

In many cases *f, g, h* profiles can be described by Voigtian functions. When using pseudoVoigt functions ($x = 2q - 2q_0$ *or* $d^* - d^*_{hkl}$):

$$pV(x) = I_o \left[(1-h)\cdot \exp\left(-\frac{p\,x^2}{b^2} \right) + h \cdot \frac{1}{1+\frac{p^2 x^2}{b^2}} \right]$$

For the ***g*** (instrumental) profile, mixing parameter (h) and width (b) can be parameterized as:

$$FWHM = \left(U \tan^2 q + V \tan q + W \right)^{1/2}$$

$$h = a + b \cdot q + c q^2$$

ANALYTICAL PROFILE FITTING

NIST SRM 1976 alumina
XRD-1 beamline
(LNLS, Campinas, Brazil)

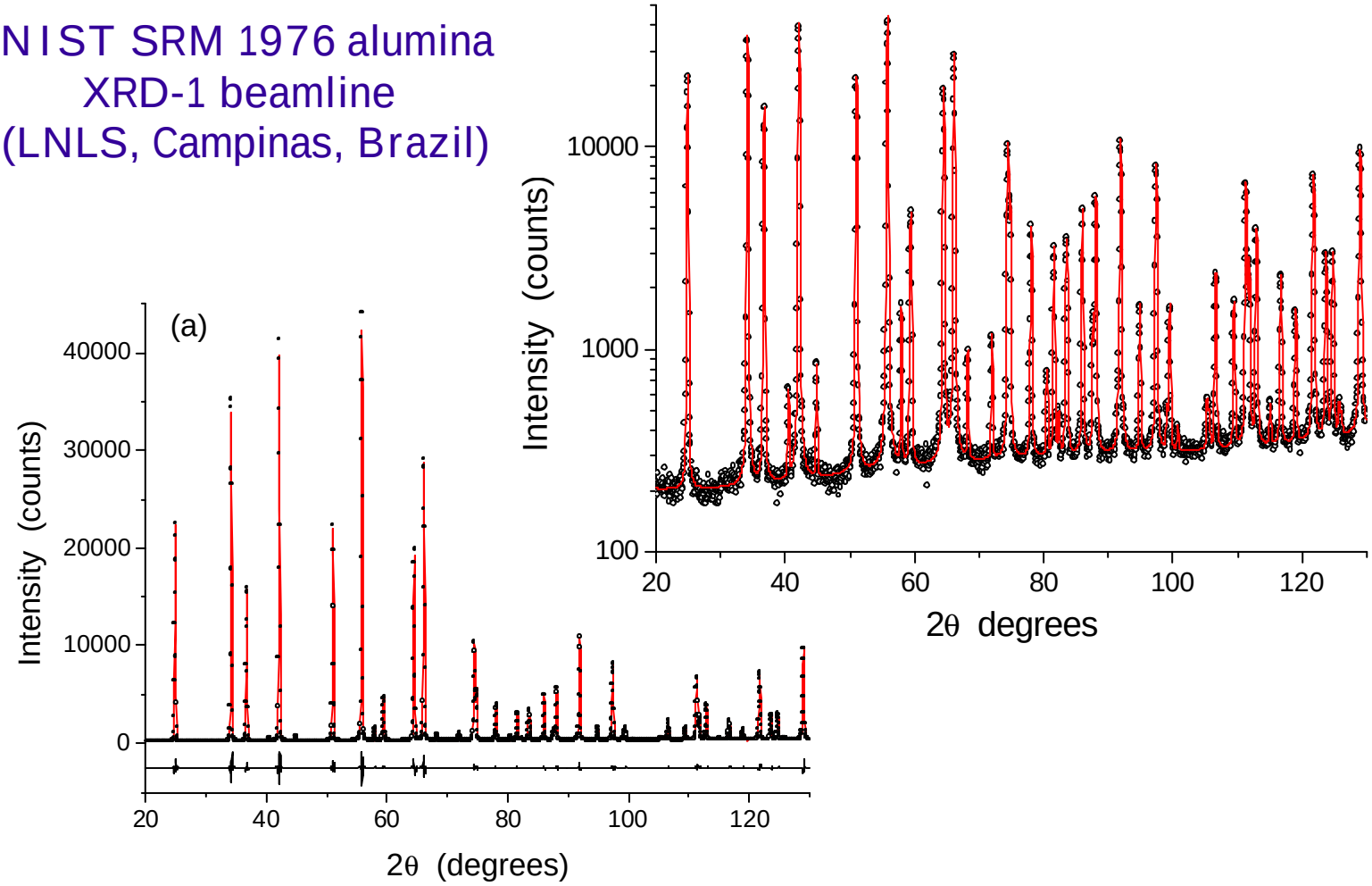

ANALYTICAL PROFILE FITTING

XRDLab at Trento. Rigaku PMG/VH: instrumental (g) profile

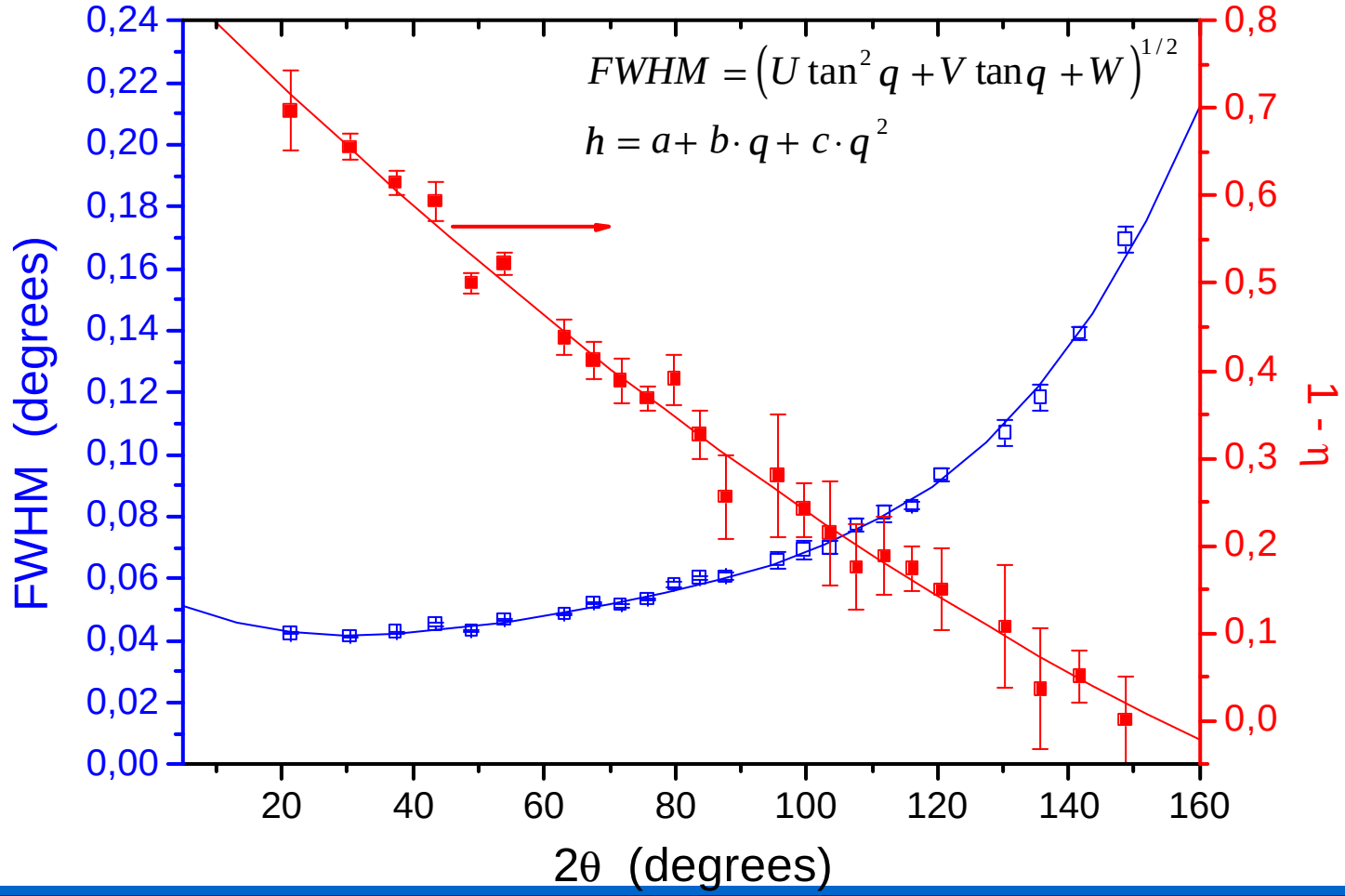

ANALYTICAL PROFILE FITTING

If both ***f*** and ***g*** profile components are assumed to be Voigtian, the ***h*** profile is also Voigtian and is given by:

$$b_{hC} = b_{gC} + b_{fC}$$

$$b_{hG} = \sqrt{b_{gG}^2 + b_{fG}^2}$$

If ***g*** is known, fitting the experimental ***h*** profile allows one to obtain the ***f*** profile:

$$b_f = (1-h)\, b_{fG} + h\, b_{fC}$$

The integral breadth of the 'true' profile (***f***) can be used, e.g., with the Scherrer formula:

L=Na

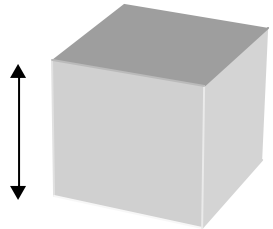

$$b_f \propto \frac{l}{L \cdot \cos q}$$

ABERRATIONS OF THE POWDER GEOMETRY

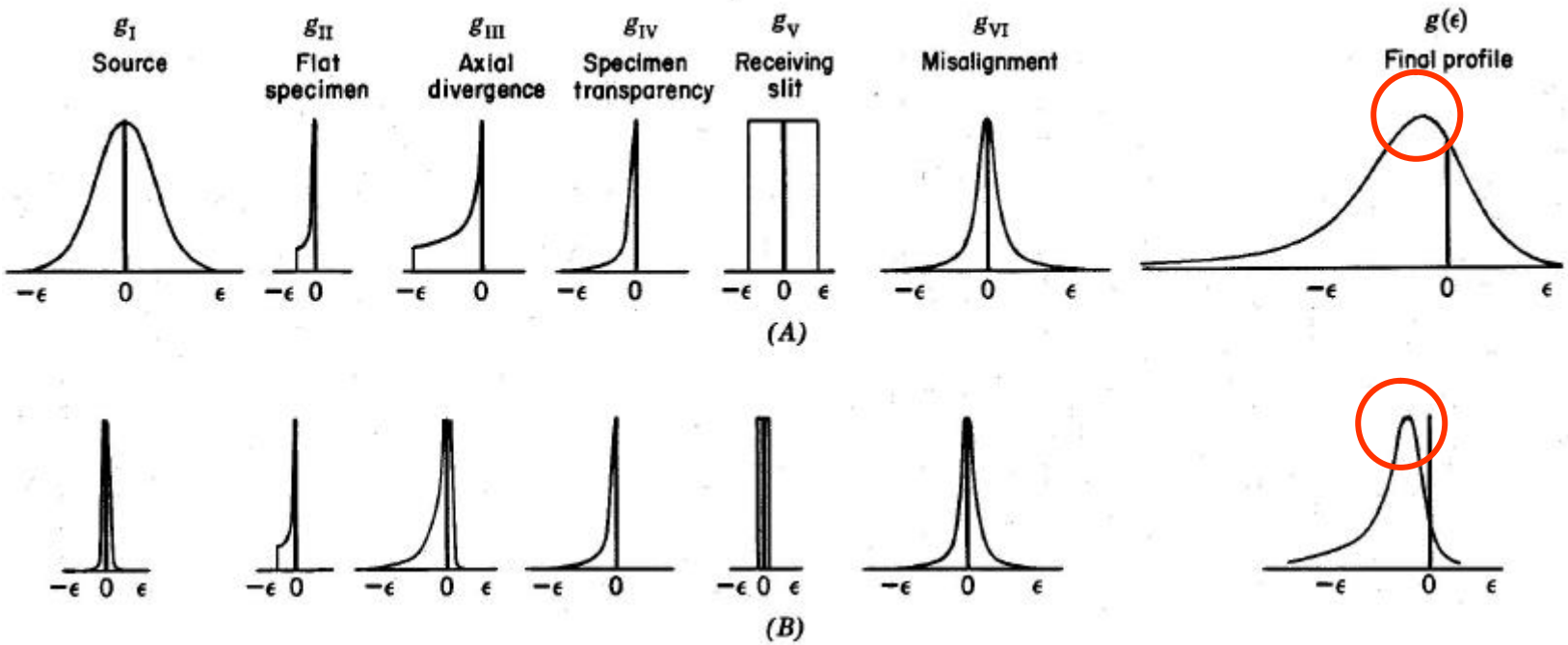

$$g = g_I \otimes g_{II} \otimes g_{III} \otimes g_{IV} \otimes ....$$

ABERRATIONS OF THE POWDER GEOMETRY

Analytical expressions of peak position aberrations.

	Centroid aberration	Parameters
Sample displacement	$\frac{-2d\cos q}{R}$	d - sample displacement R - goniometer radius
Flat specimen	$-\frac{1}{6}a^2\cot q$	α - divergence slit
Sample transparency	$\frac{-\sin(2q)}{2mR}$	μ - linear absorption coeff. R - goniometer radius
Axial Divergence	$-\frac{1}{6}d^2\cot(2q)$	δ - Soller slit (half aperture)
Refraction	$2(1-r)\tan q$	R - index of refraction
Polarization	$\frac{2W\tan q}{d^2}$	W - (°) d - interplanar spacing
Lorentz Factor and Dispersion	$\frac{3W\tan^3 q}{l^2}$	W - (°) λ - wavelength

(°) As an estimate of W, Wilson suggests to use 1/3 of the square of the doublet separation.

ABERRATIONS OF THE POWDER GEOMETRY

Shift of ***sample position*** with respect to the goniometer axis

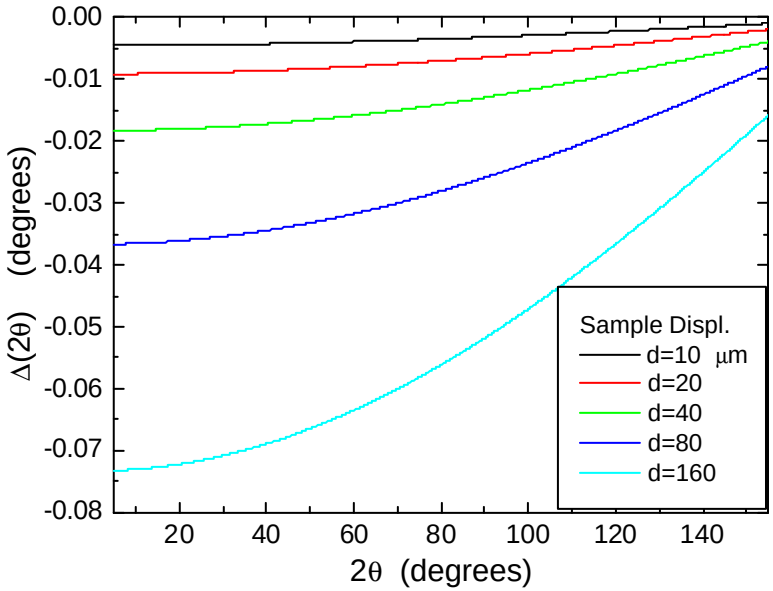

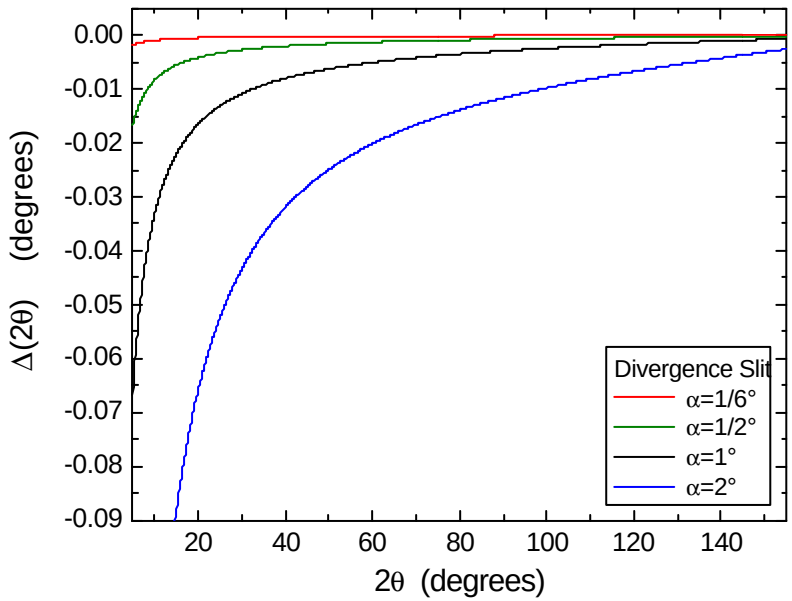

Width of the ***divergence slit***

ABERRATIONS OF THE POWDER GEOMETRY

Sample transparency

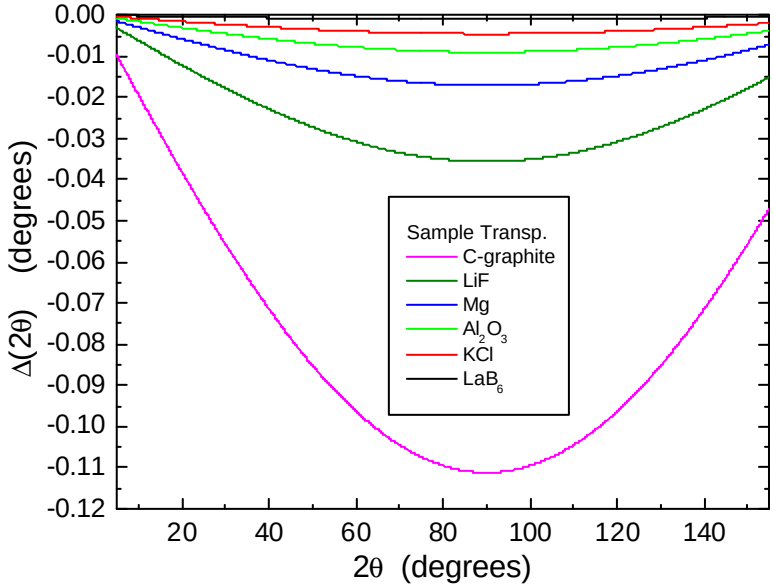

Axial divergence

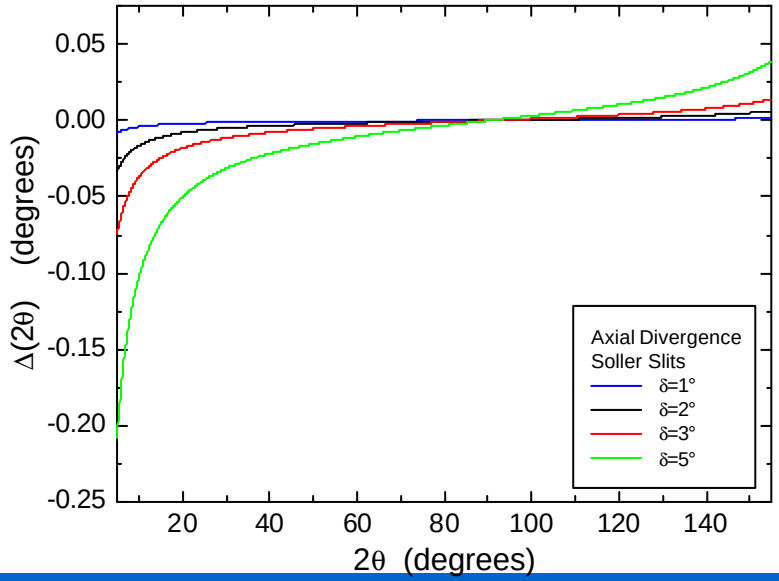

ABERRATIONS OF THE POWDER GEOMETRY

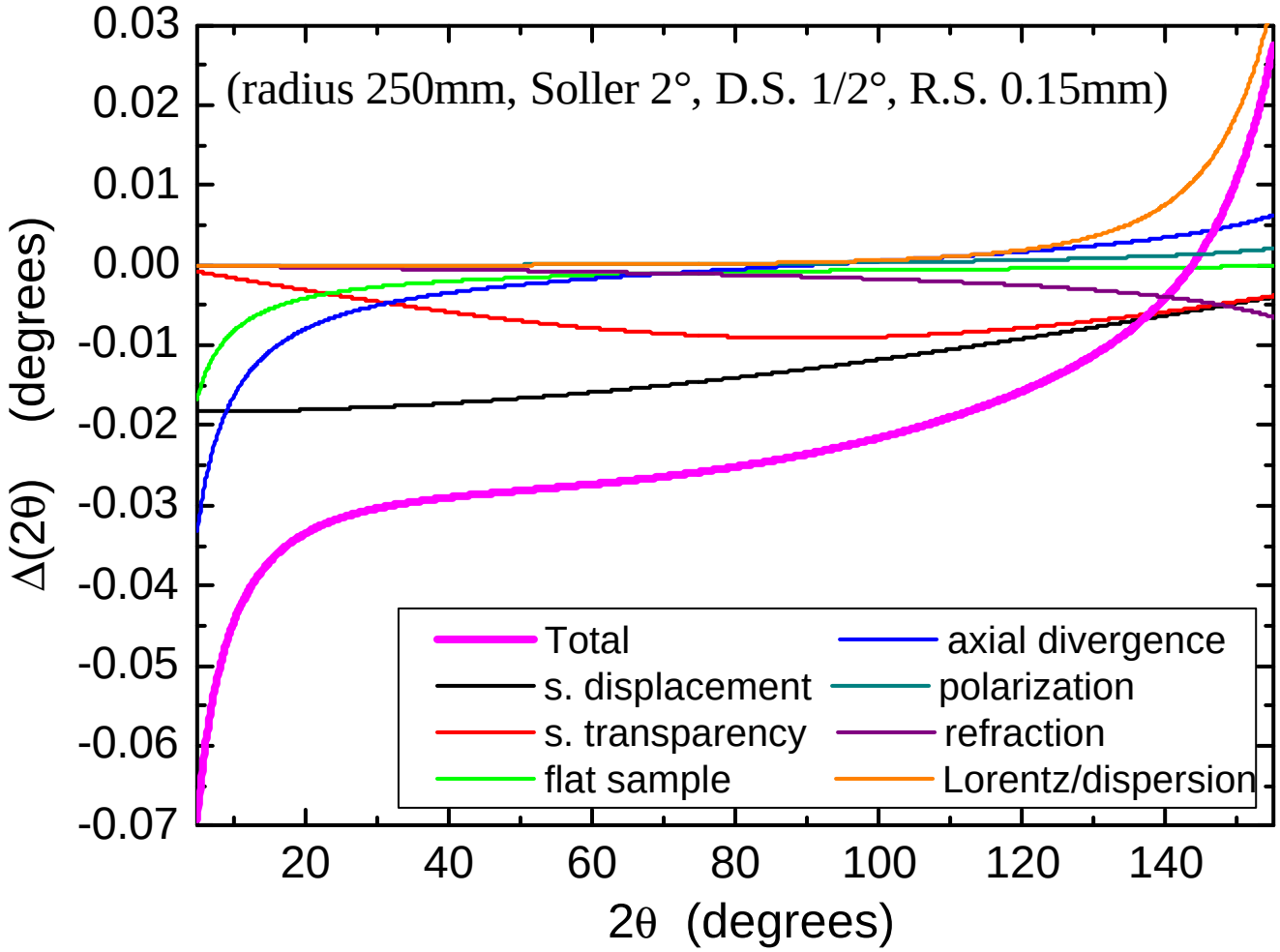

ABERRATIONS OF THE POWDER GEOMETRY

Errors in peak positions: NIST SRM 1976 alumina. D.S. ½° or 1°. Other parameters are the same (radius 250mm, Soller 2°, R.S. 0.15mm).

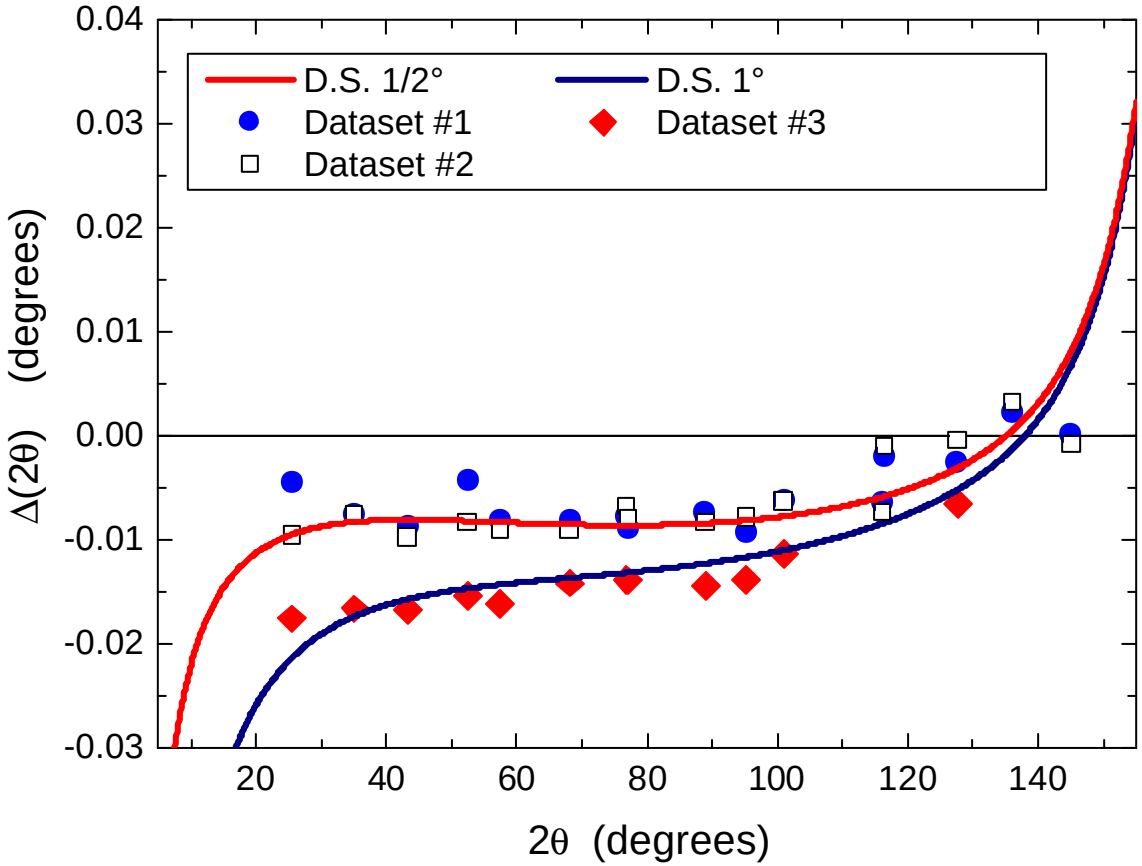

COUNTING STATISTICS

Like many natural phenomena related to the generation of random events with a finite time average, X-ray emission follows the POISSON statistics

$$p(n) = \frac{N^n}{n!} e^{-N}$$

where *n* is a positive integer. *N* is the ***mean value***:

$$\overline{n} = \sum_{n=0}^{\infty} np(n) = \sum_{n=0}^{\infty} N \frac{N^{n-1}}{(n-1)!} e^{-N} = Ne^{-N}e^{N} = N$$

If *N* is the mean value of the counts collected for a certain time, the ***standard deviation*** s_n is obtained from:

$$s_n^2 = \overline{(n-N)^2} = \overline{(n^2 + N^2 - 2nN)} = N^2 + N - N^2 = N$$

COUNTING STATISTICS

The ***standard deviation*** is given by

$$s_n = \sqrt{N}$$

And the ***relative standard deviation*** is:

$$s_{n,rel} = \frac{\sqrt{N}}{N} = \frac{1}{\sqrt{N}}$$

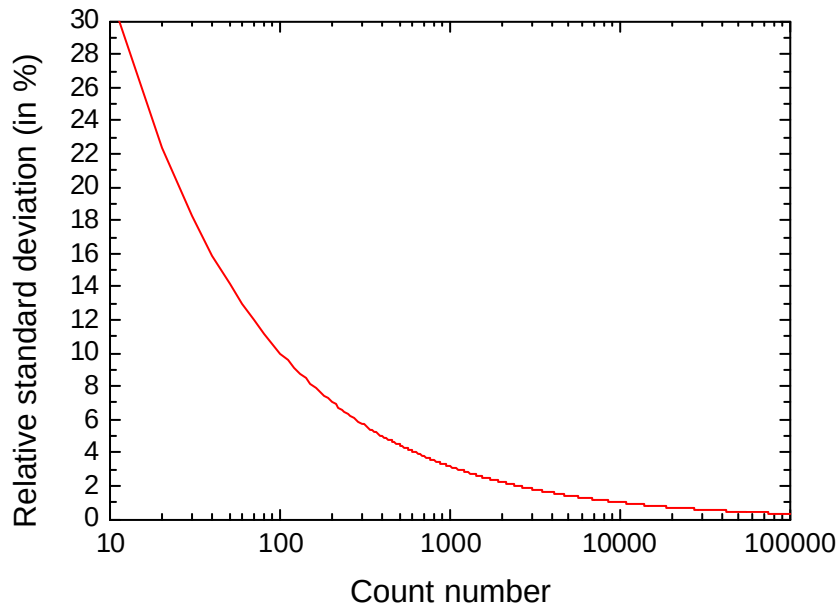

COUNTING STATISTICS

When a background is present with N_B counts, if $N_T = N_P + N_B$ is the total counts (N_P is the net peak area, with background subtracted), the relative standard deviation (in percentage) is:

$$s_P = \frac{\sqrt{N_T + N_B}}{N_T - N_B} x100$$

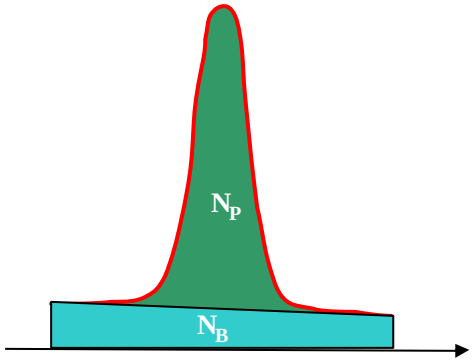

The signal-to-noise ratio, R, is defined as: $R = N_T / N_B$

$$s_P = \frac{1}{R-1}\sqrt{\frac{R(R+1)}{N_T}} x100$$

COUNTING STATISTICS

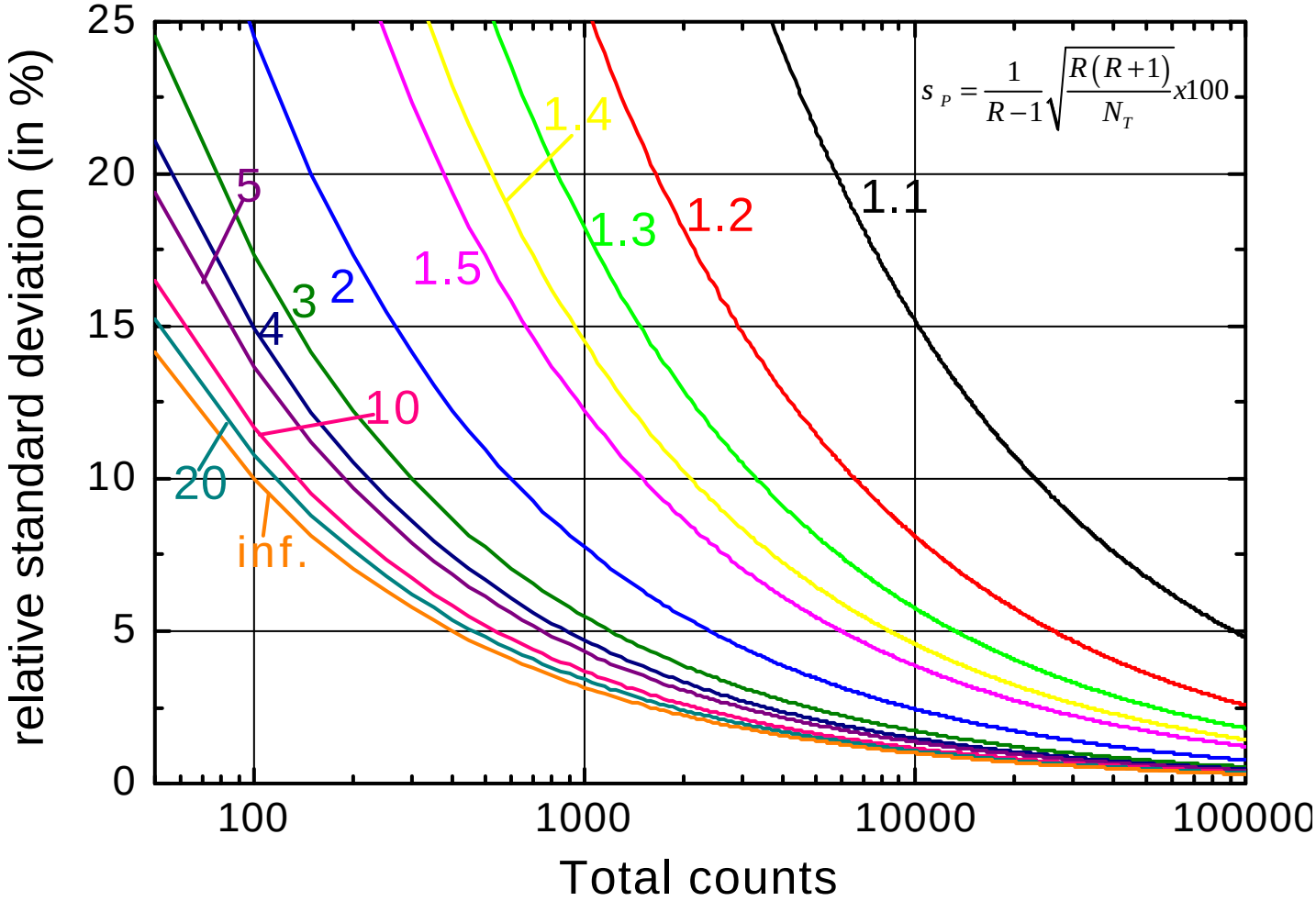

GRAIN STATISTICS

An implicit assumption of all the above reasoning is that the powder sample is homogeneous, even on a microscopic level. This is just an approximation, because samples are made of finite size grains.

If grains (actually, crystalline domains) are not sufficiently small, the concept of powder tends to lose its meaning, in the sense that it is not true anymore that for any direction there is a sufficiently large number of domains with atomic planes in Bragg conditions.

Depending on the absorption coefficient, the critical threshold for the domain size changes. In particular, the problem of having sufficiently small grains is critical for highly absorbing materials.

GRAIN STATISTICS

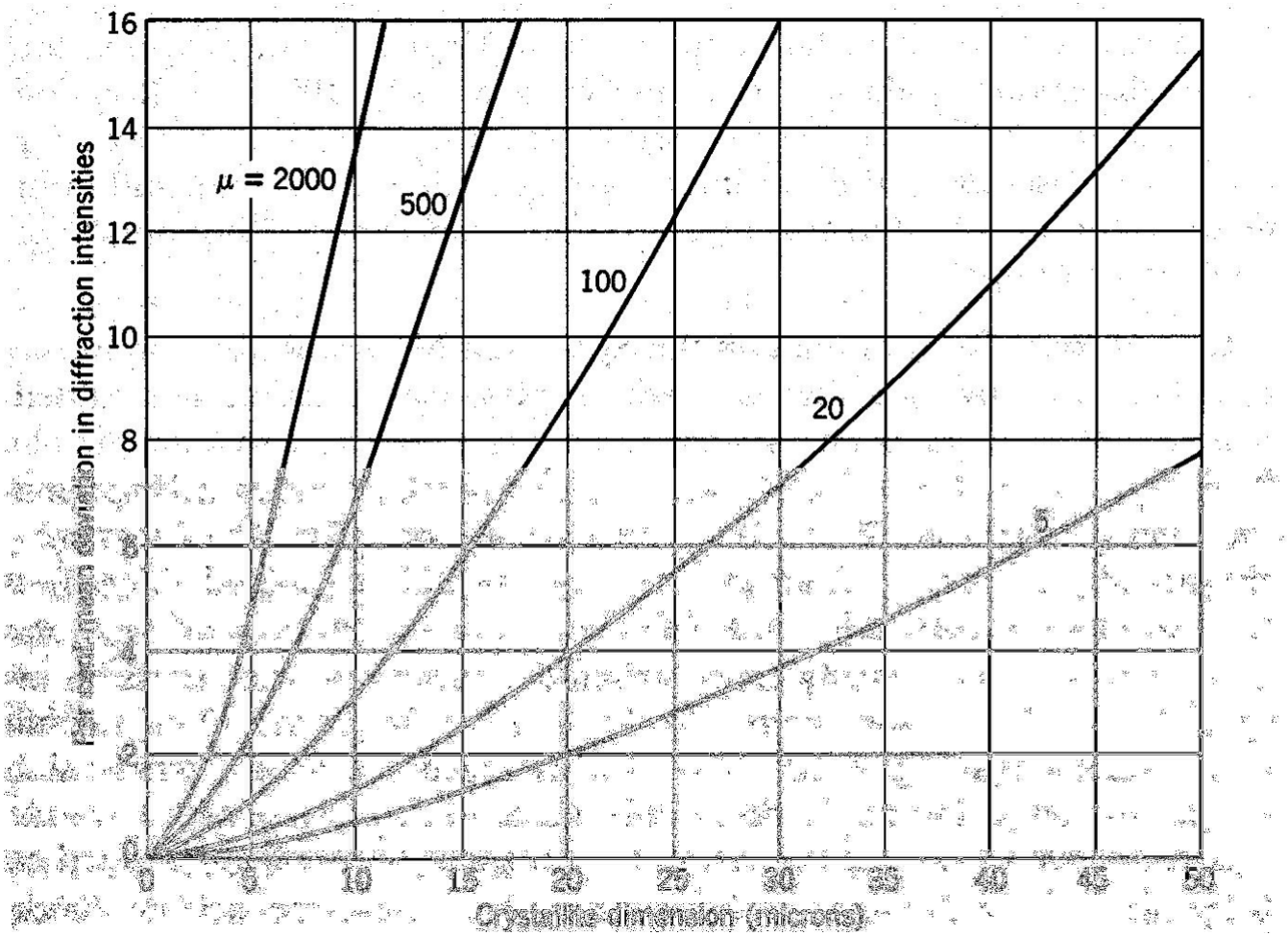

GRAIN STATISTICS

The figure below shows the intensity collected for the same reflection of quartz for different specimens of the same powder sample (from 1 to 10), prepared by selecting different granulometric fractions. The smallest deviations are obtained below 5 mm.

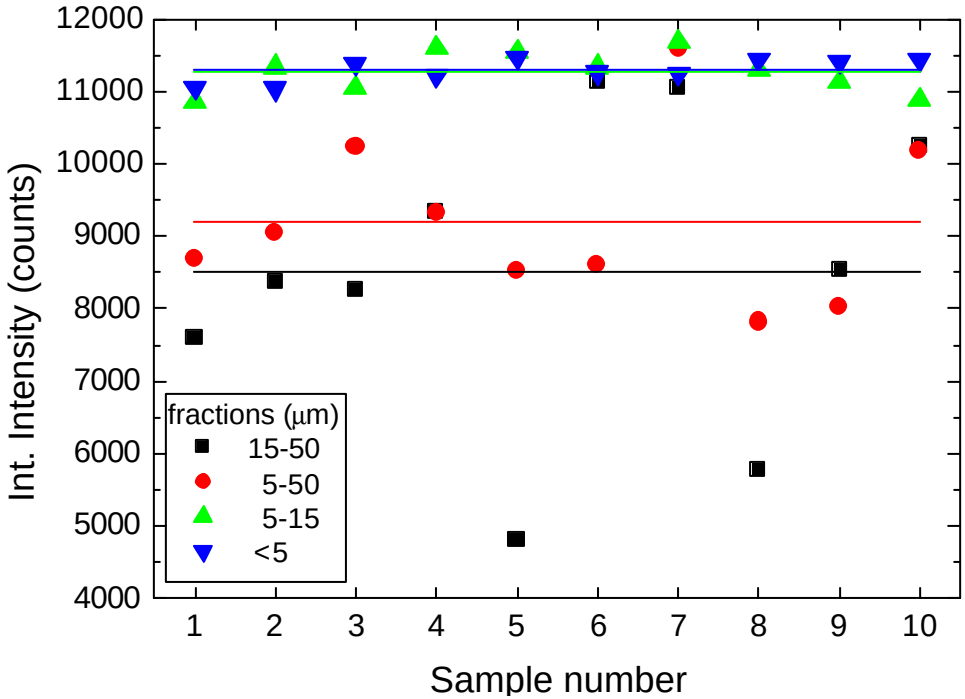

GRAIN STATISTICS

The data shown before also reveal a further effect. For the large grains, the decrease in intensity caused by absorption is increased by the fact that the fraction of diffracted intensity is also larger for these grains. Consequently, the signal is lower than that given by the same volume made of smaller (less absorbing) grains.

Mean values and standard deviations for the data of previous Figure

	15-50 μm	5-50 μm	5-15 μm	<5 μm
Mean	8512	9207	11267	11293
Standard deviation	2081 (24%)	1163 (13%)	293 (2.6%)	157 (1.4%)

This effect (extintion), together with *microabsorption* is one of the factors limiting the reliability of powder diffraction measurements. It is a particularly critical issue in *quantitative phase analysis*.

REFERENCES

References

[1] G. Hölzer, M. Fritsch, M. Deutsch, J. Härtwig & E. Förster, *Phys. Rev. A* **56** (1997) 4554-4568.

[2] S.I. Salem & P.L. Lee, *At. Data Nucl. Data Tables* **18** (1976) 234-240.

[3] NIST – National Institute of Standard and Technology, Gaithersburg, MA, USA; http://www.nist.gov

[4] J. Bergmann, R. Kleeberg, A. Haase & B. Breidenstein, *Mat. Sci. Forum* **347-349** (2000) 303-308.

[5] TOPAS, Bruker AXS, 2000. http://www.bruker-axs.com

[6] Y.H. Dong and P. Scardi, *J. Applied Crystallography* **33** (2000) 184-189.

[7] R.W. Cheary & A.A. Coelho, *J. Applied Crystallography* **25** (1992) 109-121; R.W. Cheary & A.A. Coelho, *Powder Diffraction* **13** (1998) 100-107.

[8] H.P. Klug & L.E. Alexander, *X-ray Diffraction procedures*, Wiley, New York, 1974.

[9] A.J.C. Wilson, *Mathematical Theory of X-ray Powder Diffractometry*, Philips Technical Library, Eindhoven, The Netherlands, 1963.

[10] G.K. Wertheim, M.A. Butler, K.W. West & D.N.E. Buchanan, *Rev. Sci. Instrum.* **45** (1974) 1369-1371.

[11] R.A. Young, *The Rietveld method*, Oxford University Press, Oxford, 1993.

[12] P. Scardi & M. Leoni, *J. Applied Crystallography* **32** (1999) 671-682.

[13] I.J. Langford, *J. Applied Crystallography* **11** (1978) 10-14.

[14] M. Leoni, P. Scardi, I.J. Langford, *Powder Diffraction* **13** (1998) 210-215.

[15] I.J. Langford, in *Accuracy in Powder Diffraction* II, NIST Special Publication 846, edited by E. Prince & J.K. Stalick, pp. 110-126. Washington: USG Printing Office, 1992.

[16] M. Ahtee, L. Unonius, M. Nurmela, P. Suortti, *J. Applied Crystallography* **17** (1984) 352-258.

[17] L.B. McCusker, R.B. Von Dreele, D.E. Cox, D. Louër, P. Scardi, *J. Applied Crystallography* **32** (1999) 36-50.

CONTENTS

PART I

- From single-crystal to powder diffraction
- Intensity scattered from a powder sample

PART II

- Features and aberrations of the powder geometry
- Structure factor and intensity calculations

STRUCTURE FACTOR CALCULATION

Primitive cell (*P*) (Z=1) with one atomic species only

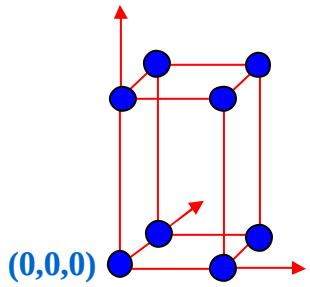

$$F = fe^{2pi(0\cdot h+0\cdot k+0\cdot l)} = f$$

$$I \propto |F|^2 = f^2$$

The structure factor is the same for all (*hkl*) refections

STRUCTURE FACTOR CALCULATION

Body centred lattice (*I*) (Z=2) with one atomic species only in (0,0,0) and (½,½,½)

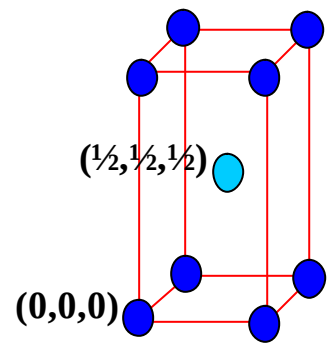

$$F = fe^{2pi(0)} + fe^{2pi(h/2+k/2+l/2)} = f\left[1+e^{pi(h+k+l)}\right] = \begin{cases} 0 & h+k+l \quad odd \\ 2f & h+k+l \quad even \end{cases}$$

The intensity is proportional to $4f^2$ for reflections with even sum of indices, and it is *zero* for those with odd sum of indices

STRUCTURE FACTOR CALCULATION

Face centred lattice (*F*) (Z=4) with one atomic species only in (0,0,0), (0,½,½), (½,0,½) and (½,½,0)

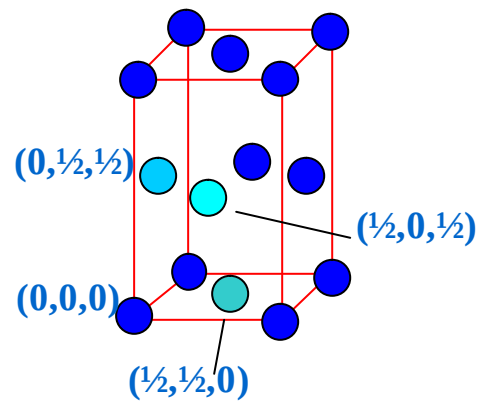

$$F = fe^{2pi(0)} + fe^{2pi(0+k/2+l/2)} + fe^{2pi(h/2+0+l/2)} + fe^{2pi(h/2+k/2+0)}$$

$$= f\left[1 + e^{pi(k+l)} + e^{pi(h+l)} + e^{pi(h+k)}\right] = \begin{cases} 0 & h,k,l \quad mixed \\ 4f & h,k,l \quad unmixed \end{cases}$$

The intensity of proportional to $16f^2$ for reflections with mixed indices and it is *zero* for those with unmixed indices

STRUCTURE FACTOR CALCULATION

P	*I*	*F*
(100)	-	-
(110)	(110)	-
(111)	-	(111)
(200)	(200)	(200)
(210)	-	-
(211)	(211)	-
(220)	(220)	(220)
(300)/(221)	-	-
(310)	(310)	-
(311)	-	(311)
(222)	(222	(222)
(320)	-	-
(321)	(321)	-
(400)	(400)	(400)

The structure factor is independent of *shape* and *size* of the unit cell.

Rules shown in the previous examples are then valid for any *P*, *I*, *or F* cells.

EXAMPLE

Calculated integrated intensity
for the reflections of Fluorite

FLUORITE POWDER PATTERN

Fluorite (CaF_2): ***fcc*** (Z=4) unit cell.

Cations (Ca^{+2}, r=0.99 Å) in the origin and positions equivalent by *fcc* Translations.

Anions (F^{-1}, R=1.33 Å) in (¼,¼,¼), (¼,¼,¾) and positions equivalent by *fcc* Translations.

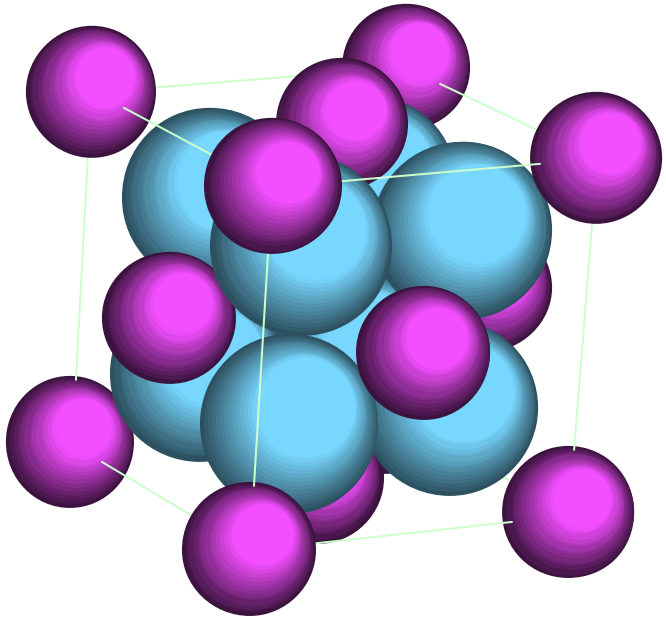

FLUORITE POWDER PATTERN

Ca^{+2} (0,0,0) + *fcc*

F^{-1} (¼,¼,¼), (¼,¼,¾) + *fcc*.

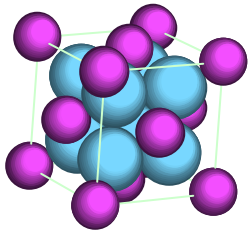

$$F = 4\left[f_{Ca} + f_F e^{\frac{ip}{2}(h+k+l)} + f_F e^{\frac{ip}{2}(h+k+3l)} \right] = 4\left[f_{Ca} + f_F \left(e^{\frac{ip}{2}(h+k+l)} + e^{\frac{ip}{2}(h+k-l)} \right) \right] =$$

$$= 4\left[f_{Ca} + 2 f_F e^{\frac{ip}{2}(h+k)} \cos\left(\frac{pl}{2} \right) \right]$$

$$|F|^2 = 16\left\{ f_{Ca}^2 + 4 f_F^2 \cos^2\left(\frac{pl}{2} \right) + 4 f_{Ca} f_F \left[e^{\frac{ip}{2}(h+k)} + e^{-\frac{ip}{2}(h+k)} \right] \cos\left(\frac{pl}{2} \right) \right\} =$$

$$= 16\left\{ f_{Ca}^2 + 4 f_F^2 \cos^2\left(\frac{pl}{2} \right) + 4 f_{Ca} f_F \cos\left[\frac{p}{2}(h+k) \right] \cos\left(\frac{pl}{2} \right) \right\}$$

FLUORITE POWDER PATTERN

$$|F|^2 = 16\left\{ f_{Ca}^2 + 4 f_F^2 \cos^2\left(\frac{pl}{2}\right) + 4 f_{Ca} f_F \cos\left[\frac{p}{2}(h+k)\right]\cos\left(\frac{pl}{2}\right)\right\}$$

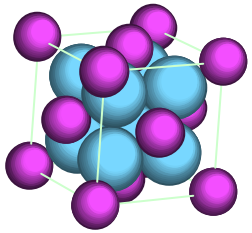

The expression simplifies consideraning that *h,k,l* are integers:

$$|F|_A^2 = 16 f_{Ca}^2 \qquad l \text{ odd}$$

$$|F|_B^2 = 16\left(f_{Ca} - 2 f_F \right)^2 \qquad (h+k) \textit{ or } l \text{ odd } \textit{multiple} \text{ of } 2$$

$$|F|_C^2 = 16\left(f_{Ca} + 2 f_F \right)^2 \qquad (h+k) \text{ and } l\text{, both odd or both even multiple of } 2$$

(111)	(200)	(220)	(311)	(222)	(400)	(331)	(420)	(422)	(333)	(511)	(440)	(531)	(600)
$\lvert F\rvert_A^2$	$\lvert F\rvert_B^2$	$\lvert F\rvert_C^2$	$\lvert F\rvert_A^2$	$\lvert F\rvert_B^2$	$\lvert F\rvert_C^2$	$\lvert F\rvert_A^2$	$\lvert F\rvert_B^2$	$\lvert F\rvert_C^2$	$\lvert F\rvert_A^2$	$\lvert F\rvert_A^2$	$\lvert F\rvert_C^2$	$\lvert F\rvert_A^2$	$\lvert F\rvert_B^2$

FLUORITE POWDER PATTERN

$$|F|_A^2 = 16 f_{Ca}^2 \qquad l \text{ odd}$$

$$|F|_B^2 = 16(f_{Ca} - 2 f_F)^2 \qquad (h+k) \text{ or } l \text{ odd multiple of } 2$$

$$|F|_C^2 = 16(f_{Ca} + 2 f_F)^2 \qquad (h+k) \text{ and } l, \text{ both odd or both even multiple of } 2$$

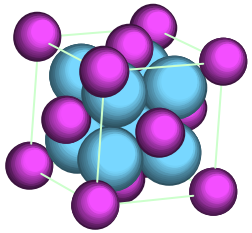

Atomic scattering factor (*f*):

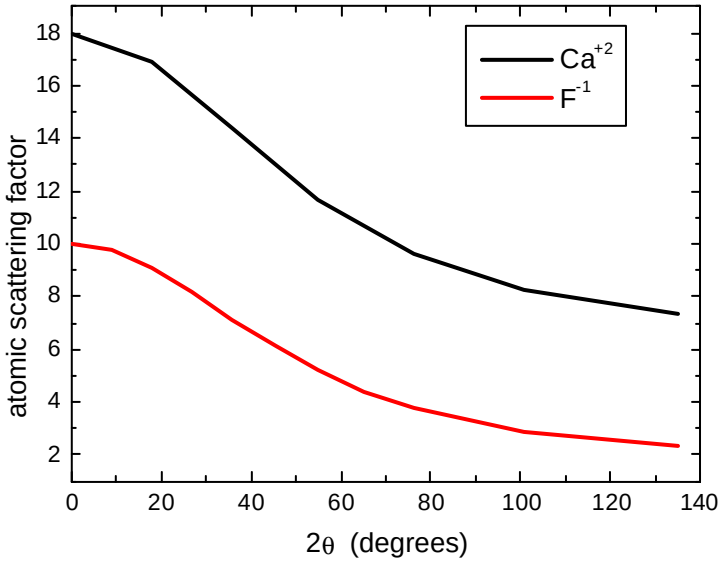

Dispersion corrections:

	Ca	F
$\Delta f'$	0.3	0.0
$\Delta f''$	1.4	0.1

→ $(f + \Delta f') + i \Delta f''$

Debye-Waller factors:

$$B(Ca) = 0.47\ \text{Å}^2,\ B(F) = 0.67\ \text{Å}^2$$

FLUORITE POWDER PATTERN

$$|F|_A^2 = 16 f_{Ca}^2 \qquad l \text{ odd}$$

$$|F|_B^2 = 16\left(f_{Ca} - 2 f_F\right)^2 \qquad (h+k) \text{ or } l \text{ odd multiple of } 2$$

$$|F|_C^2 = 16\left(f_{Ca} + 2 f_F\right)^2 \qquad (h+k) \text{ and } l\text{, both odd or both even multiple of } 2$$

(f+Df')+iDf"

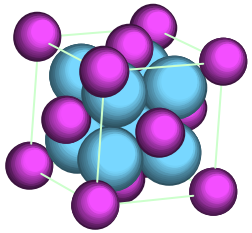

$$|F_T|_A^2 = 16 f_{Ca}^2 e^{-2M_{Ca}} = 16\left[\left(f_{0,Ca} + \Delta f'_{Ca}\right)^2 + \left(\Delta f''_{Ca}\right)^2\right] e^{-2M_{Ca}}$$

$$|F_T|_B^2 = 16\left(f_{Ca} e^{-M_{Ca}} - 2 f_F e^{-M_F}\right)^2 =$$

$$= 16\left\{\left[\left(f_{0,Ca} + \Delta f'_{Ca}\right) e^{-M_{Ca}} - 2\left(f_{0,F} + \Delta f'_F\right) e^{-M_F}\right]^2 + \left(\Delta f''_{Ca} e^{-M_{Ca}} - 2\Delta f''_F e^{-M_F}\right)^2\right\}$$

$$|F_T|_C^2 = 16\left(f_{Ca} e^{-M_{Ca}} + 2 f_F e^{-M_F}\right)^2 =$$

$$= 16\left\{\left[\left(f_{0,Ca} + \Delta f'_{Ca}\right) e^{-M_{Ca}} + 2\left(f_{0,F} + \Delta f'_F\right) e^{-M_F}\right]^2 + \left(\Delta f''_{Ca} e^{-M_{Ca}} + 2\Delta f''_F e^{-M_F}\right)^2\right\}$$

FLUORITE POWDER PATTERN

$$|F|_A^2 = 16 f_{Ca}^2 \qquad l \text{ odd}$$

$$|F|_B^2 = 16(f_{Ca} - 2 f_F)^2 \qquad (h+k) \text{ or } l \text{ odd } \textit{multiple} \text{ of } 2$$

$$|F|_C^2 = 16(f_{Ca} + 2 f_F)^2 \qquad (h+k) \text{ and } l, \text{ both odd or both even multiple of } 2$$

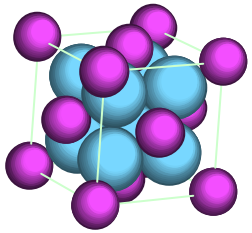

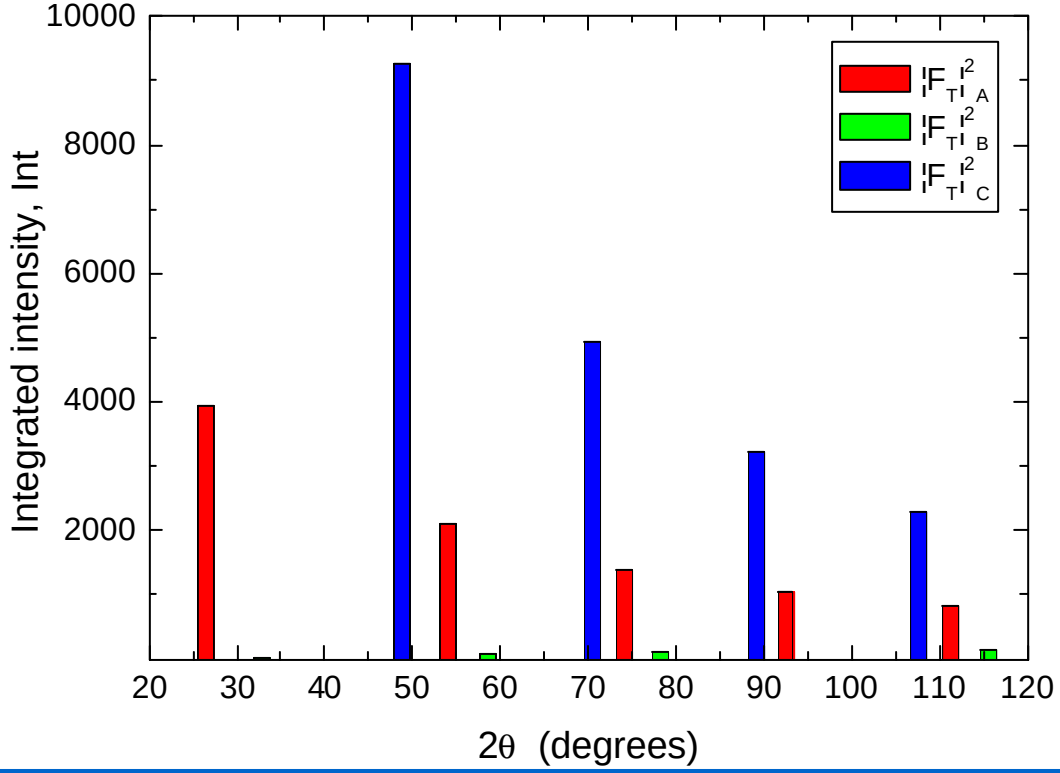

FLUORITE POWDER PATTERN

$$|F|_A^2 = 16 f_{Ca}^2 \qquad l \text{ odd}$$

$$|F|_B^2 = 16\left(f_{Ca} - 2 f_F\right)^2 \qquad (h+k) \text{ or } l \text{ odd } \textit{multiple} \text{ of } 2$$

$$|F|_C^2 = 16\left(f_{Ca} + 2 f_F\right)^2 \qquad (h+k) \text{ and } l, \text{ both odd or both even multiple of } 2$$

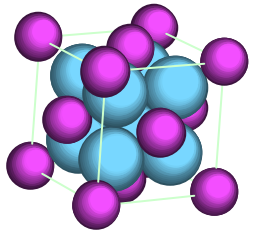

hkl	$2q$	$\sin q/l$	LP	p	$e^{-B(Ca)\frac{\sin^2 q}{l^2}}$	$e^{-B(F)\frac{\sin^2 q}{l^2}}$	$e^{-\bar{B}\frac{\sin^2 q}{l^2}}$	$f_{0,Ca^{+2}}$	$f_{0,F^{-1}}$	$\lvert F_T\rvert_A^2$	$\lvert F_T\rvert_B^2$	$\lvert F_T\rvert_C^2$	Int (§)	Int' (#)
111	28.27	0.1585	15.00	8	0.988	0.983	0.985	15.53	7.99	3947			**86.3**	86.3
200	32.76	0.1830	10.94	6	0.984	0.978	0.979	14.87	7.49		24		**0.3**	0.3
220	47.00	0.2588	4.94	12	0.969	0.956	0.959	12.77	5.93			9259	**100.0**	100.0
311	55.76	0.3035	3.36	24	0.958	0.940	0.944	11.61	5.12	2109			**31.0**	30.4
222	58.48	0.3171	3.02	8	0.954	0.935	0.940	11.28	4.90		79		**0.3**	0.3
400	68.67	0.3661	2.14	6	0.939	0.914	0.920	10.22	4.18			4950	**11.6**	11.5
331	75.85	0.3989	1.77	24	0.928	0.899	0.906	9.62	3.79	1382			**10.7**	10.3
420	78.18	0.4093	1.68	24	0.924	0.894	0.901	9.45	3.68		114		**0.8**	0.7
422	87.37	0.4483	1.45	24	0.910	0.874	0.883	8.87	3.31			3228	**20.5**	20.1
333 511	94.22	0.4756	1.38	8 24	0.899	0.859	0.869	8.52	3.07	1032 1032			**2.1** **6.2**	1.9 5.8
440	105.8	0.5177	1.39	12	0.882	0.836	0.847	8.03	2.71		0	2288	**7.0**	6.8
531	113.06	0.5415	1.49	48	0.871	0.822	0.834	7.76	2.50	812			**10.6**	9.8
600	115.57	0.5492	1.54	6	0.868	0.817	0.829	7.67	2.44	0	155		**0.3**	0.2

$a_0 = 5.463$Å $\quad q_m = 13.28°$ $\quad M = B(\sin q/l)^2$ $\quad l = 1.540598$Å

FLUORITE POWDER PATTERN

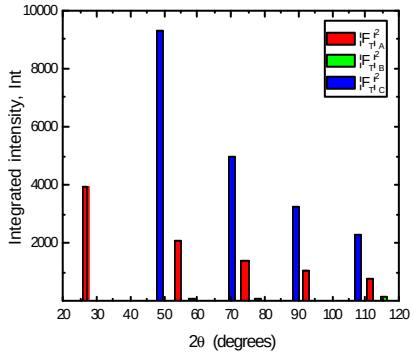

Experimental pattern of fluorite powder

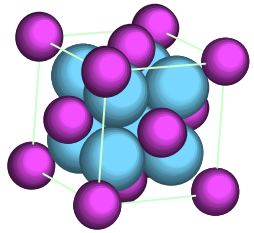

a_0	sd	R_{wp}	R_{exp}	GoF
5.4639 (1) Å	11 μm	23.98 %	22.33	1.074

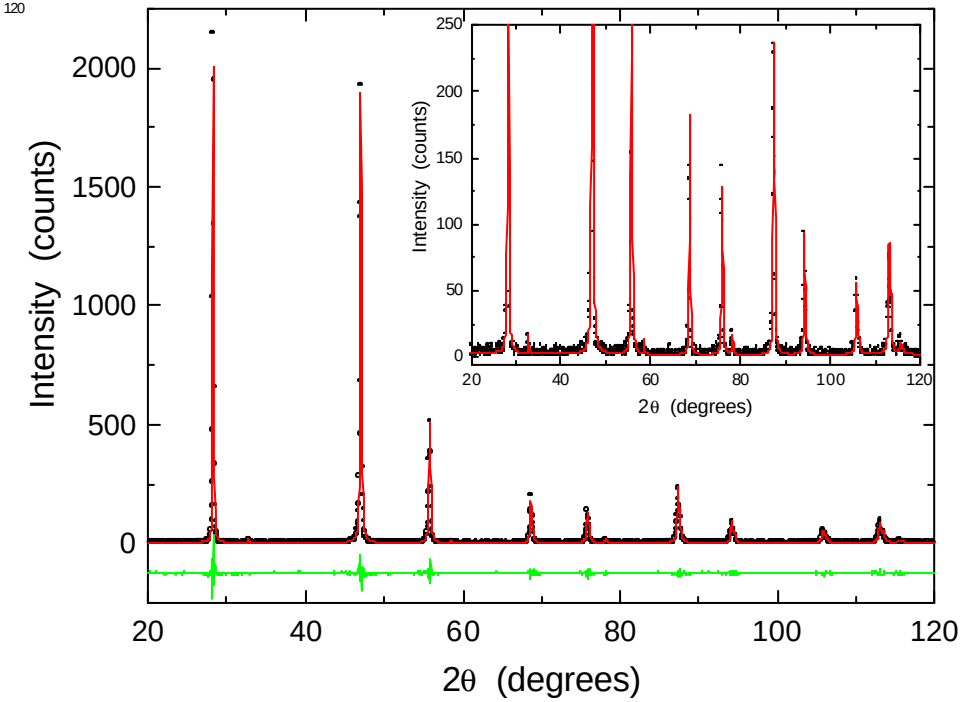

FLUORITE POWDER PATTERN

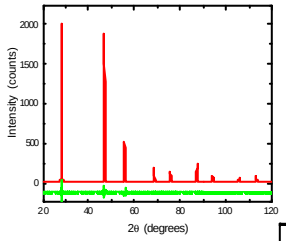

Experimental pattern of fluorite powder: profile fitting results

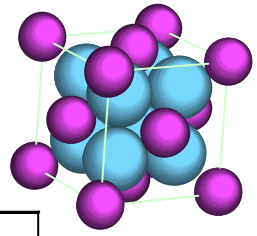

(hkl)	$2q$	d_{hkl}	I_{max}	*Area*	*Int*	$HWHM_f$	h_f	$HWHM_h$	h_h
111	28.267	3.1546	1676 (25)	318.5	**83.66**	0.0619 (0.0015)	0.41 (0.02)	0.073	0.47
200	32.754	2.7320	12 (3)	1.7	**0.44**	0.051 (0.016)	0.00 (0.15)	0.061	0.15
220	47.000	1.9318	1688 (21)	379.9	**100**	0.0528 (0.0013)	1.00 (0.04)	0.074	0.91
311	55.754	1.6474	453 (13)	124.2	**32.68**	0.066 (0.006)	1.00 (0.13)	0.089	0.94
222	58.467	1.5773	10 (2)	1.5	**0.41**	0.041 (0.024)	0.23 (0.85)	0.058	0.47
400	68.654	1.3660	167 (7)	48.6	**12.78**	0.067 (0.009)	1.00 (0.21)	0.094	0.94
331	75.833	1.2535	117 (6)	42.7	**11.23**	0.088 (0.013)	1.00 (0.22)	0.118	0.96
420	78.171	1.2218	14 (2)	4.6	**1.22**	0.077 (0.045)	1.00 (0.94)	0.108	0.95
422	87.364	1.1153	221 (7)	83.6	**22.01**	0.086 (0.010)	1.00 (0.16)	0.122	0.97
333 511	94.201	1.0515	21(1) 64(14)	8.5 25.6	**2.24** **6.73**	0.089 (0.017)	1.00 (0.29)	0.129	0.97
440	105.784	0.9659	50 (3)	28.0	**7.37**	0.131 (0.026)	1.00 (0.31)	0.179	0.99
531	113.033	0.9236	79 (4)	44.3	**11.65**	0.125 (0.020)	1.00 (0.26)	0.179	0.99
600	115.532	0.9107	7 (2)	5.4	**1.42**	0.19 (0.11)	1.00 (0.93)	0.251	0.99

FLUORITE POWDER PATTERN

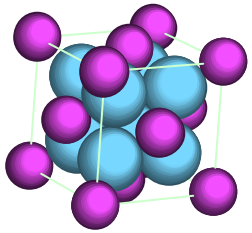

Comparison between calculated and measured integrated intensities:

hkl	2*q*	**Calculated** Integ. Int.	**Experimental** Integ. Int.
111	28.27	**86.3**	**83.7**
200	32.76	**0.3**	**0.4**
220	47.00	**100.0**	**100.0**
311	55.76	**31.0**	**32.7**
222	58.48	**0.3**	**0.4**
400	68.67	**11.6**	**12.8**
331	75.85	**10.7**	**11.2**
420	78.18	**0.8**	**1.2**
422	87.37	**20.5**	**22.0**
333 511	94.22	**2.1** **6.2**	**2.2** **6.7**
440	105.8	**7.0**	**7.4**
531	113.06	**10.6**	**11.6**
600	115.57	**0.3**	**1.4**

FLUORITE POWDER PATTERN

Counting statistics:

$$s_P = \frac{\sqrt{N_T + N_B}}{N_T - N_B} x100$$

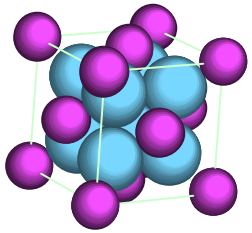

hkl	I_{rel} (%)	$2\theta_{start}$ (gradi)	$2\theta_{end}$ (gradi)	N_B (conteggi)	$N_T = N_P + N_B$ (conteggi)	s_P (%)
111	83.66	26.75	29.65	177	9452	**1.0**
200	0.44	31.45	33.90	141	224	**23.0**
220	100	45.45	48.40	141	11037	**1.0**
311	32.68	53.90	57.45	154	3770	**1.7**
222	0.41	57.25	59.55	98	243	**12.7**
400	12.78	66.70	70.45	147	1612	**2.9**
331	11.23	73.40	78.10	177	1538	**3.0**
420	1.22	75.95	80.25	161	919	**4.3**
422	22.01	84.85	89.75	182	2679	**2.1**
333/511	2.24/6.73	91.55	96.70	194	1287	**3.5**
440	7.37	102.15	109.30	286	1243	**4.1**
531	*11.65*	*109.35*	*116.55*	*306*	*1865*	***3.0***
600	*1.42*	*110.45*	*119.95*	*413*	*2014*	***3.1***

FLUORITE POWDER PATTERN

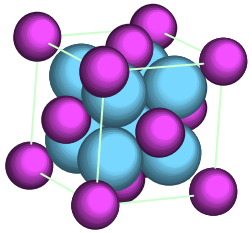

Comparison between calculated and measured integrated intensities:

hkl	2*q*	**Calculated** Integ. Int.	**Experimental** Integ. Int.	s_P (%)
111	28.27	**86.3**	**83.7**	**1.0**
200	32.76	**0.3**	**0.4**	**23.0**
220	47.00	**100.0**	**100.0**	**1.0**
311	55.76	**31.0**	**32.7**	**1.7**
222	58.48	**0.3**	**0.4**	**12.7**
400	68.67	**11.6**	**12.8**	**2.9**
331	75.85	**10.7**	**11.2**	**3.0**
420	78.18	**0.8**	**1.2**	**4.3**
422	87.37	**20.5**	**22.0**	**2.1**
333 511	94.22	**2.1** **6.2**	**2.2** **6.7**	**3.5**
440	105.8	**7.0**	**7.4**	**4.1**
531	113.06	**10.6**	**11.6**	***3.0***
600	115.57	**0.3**	**1.4**	***3.1***

FLUORITE POWDER PATTERN

Result using the Rietveld method (TOPAS ©) :

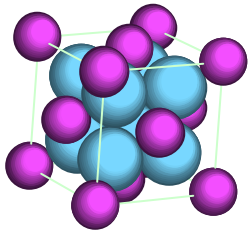

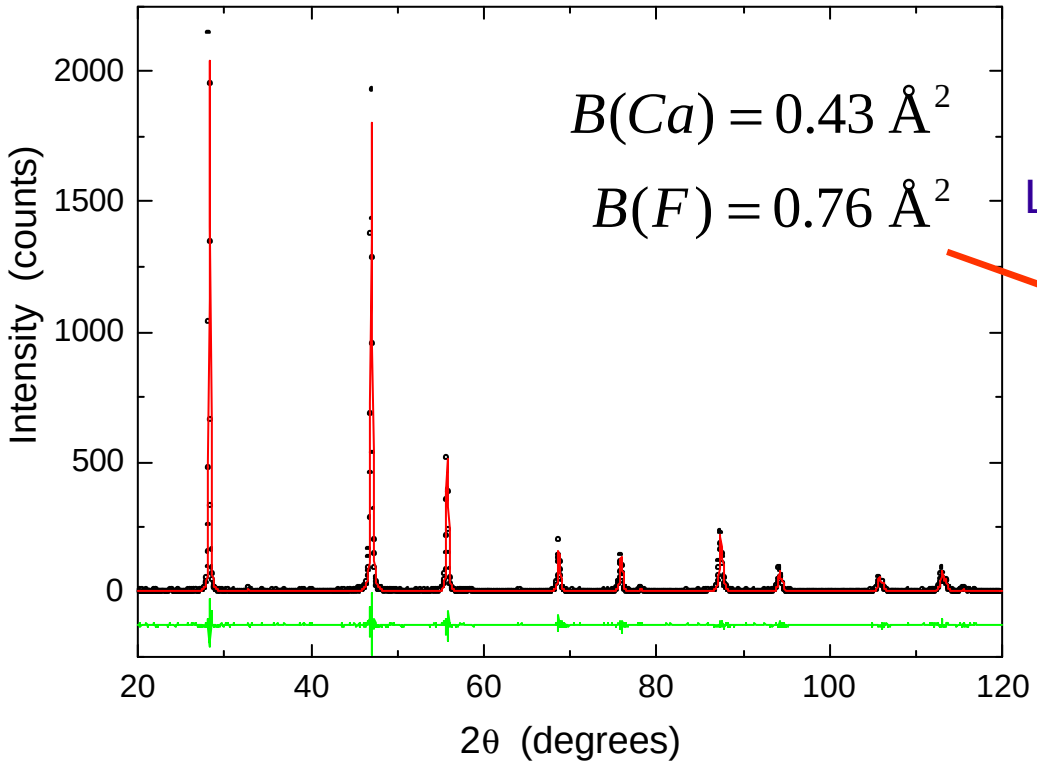

Literature values:

$B(Ca) = 0.47$ Å^2

$B(F) = 0.67$ Å^2

REFERENCES

REFERENCES

[1] International Tables for X-ray Crystallography, 3rd series. Kluwer Academic Publishers, Dordrecht, Boston, London. Vol.A (1983), Vol.B (1993), Vol.C (1992), "Brief Teaching Edition of Volume A" (1985).

[2] http://www.ccp14.ac.uk/ ; http://www.iucr.org/sincris-top/logiciel/index.html

[3] P.P. Ewald, *Fifty years of X-ray Diffraction*, Reprinted in pdf format for the IUCr XVIII Congress, Glasgow, Scotland Copyright © 1962, 1999 International Union of Crystallography, Chester, UK.

[4] B.E. Warren, *X-ray Diffraction*, Addison-Wesley, Reading, MA, 1969.

[5] I.C. Noyan & J.B. Cohen, *Residual Stress*, Springer-Verlag, New York, 1989.

[6] J.I. Langford, "Line Profiles and sample Microstructure", in *Industrial Applications of X-ray Diffraction*, edited by F.H. Chung and D.K. Smith, Marcel Dekker, New York, 2000.

[7] R.A.Young, *The Rietveld method*, Oxford University Press, Oxford, 1993.

[8] B.D. Cullity, *Elements of X-ray Diffraction*, Addison-Wesley, reading Ma, 1978.

[9] H.P. Klug & L.E. Alexander, *X-ray Diffraction procedures*, Wiley, New York, 1974.

[10] Y.H. Dong and P. Scardi, *J. Applied Crystallography* **33** (2000) 184-189.

[11] TOPAS, Bruker AXS, 2000. http://www.bruker-axs.com

[12] International Centre for Diffraction Data, Newtown Square, PA, USA. http://www.icdd.com

[13] JADE 5+. MDI, Materials Data: http://www.materialsdata.com